

# Planetary Waves on a Hemisphere Bounded by Meridians of Longitude

M. S. Longuet-Higgins

*Phil. Trans. R. Soc. Lond. A* 1966 **260**, 317-350

doi: 10.1098/rsta.1966.0053

## Email alerting service

Receive free email alerts when new articles cite this article - sign up in the box at the top right-hand corner of the article or click [here](#)

# PLANETARY WAVES ON A HEMISPHERE BOUNDED BY MERIDIANS OF LONGITUDE

By M. S. LONGUET-HIGGINS, F.R.S.

*National Institute of Oceanography, Wormley, Surrey*

(Received 4 October 1965)

## CONTENTS

	PAGE		PAGE
1. INTRODUCTION	317	7. THE EIGENVECTORS	326
2. FORMULATION OF THE PROBLEM	319	8. THE STREAMFUNCTIONS	327
3. FIRST METHOD OF SOLUTION	319	9. APPLICATION TO THE PACIFIC OCEAN	342
4. NATURE OF THE SOLUTIONS	321	10. CONCLUSIONS	344
5. METHOD OF COMPUTATION	322	APPENDIX. AN ALTERNATIVE METHOD	344
6. THE EIGENVALUES	324	REFERENCES	349

This paper studies the free modes of oscillation in a rotating hemispherical basin bounded by a great-circle passing through the pole of rotation. The radius  $R$  of the globe, the rate of rotation  $\Omega$ , the depth of fluid  $h$  and the acceleration of gravity  $g$  are assumed to be such that  $h \ll R$  and  $R\Omega/\sqrt{gh} \ll 1$ . The waves can then be treated as non-divergent. The problem is solved by two independent methods, and the results are compared with each other and with the  $\beta$ -plane approximation. It is found that the eight lowest modes of oscillation correspond quite well to simple modes in the  $\beta$ -plane, the approximate periods being within 20%. Higher modes show no clear correspondence.

It is suggested that the peak at 0.5 c/d in the spectrum of sea level at Honolulu may correspond to the lowest mode of oscillation in the Pacific Ocean.

## 1. INTRODUCTION

The question whether oscillations of fluid can exist in a rotating shell of fluid, with boundaries consisting of meridians of longitude, is of interest in connexion with the possible long-period oscillations of currents in ocean basins. Most of the classical researches on the fluid oscillations in closed basins (see, for example, Goldsbrough 1913, 1914, 1929, 1933; Proudman 1920; Proudman & Doodson 1936) have been directed to a slightly different problem, the problem of the forced response of the system to tide-raising forces, with periods of order 12 h. Here we shall be concerned with oscillations having longer periods, of the order of several days. Such oscillations might be set up by the horizontal stresses exerted on the ocean by variable winds.

It is well known from the work of Hough (1898) and others that the solutions of Laplace's tidal equations for a rotating spherical ocean are of two kinds: the short gravity waves, modified to a certain extent by the rotation, and the longer-period 'planetary waves', which are essentially currents rendered time-periodic by the rotation. It can be shown

(see Longuet-Higgins 1965) that when the parameter  $R\Omega/\sqrt{gh}$  is sufficiently small (where  $R$  is the Earth's radius,  $\Omega$  the angular rotation,  $g$  the acceleration due to gravity, and  $h$  the depth of water) then the planetary waves—though not the gravity waves—become non-divergent. Thus the motions become similar to the oscillations of fluid contained between two rigid spherical surfaces.

The nature of such oscillations in closed basins was recently investigated by an approximate method known as the  $\beta$ -plane approximation (Rattray 1964; Longuet-Higgins 1964 *a*, 1965; see also Hoiland 1950) in which the spherical surface is replaced locally by a plane, but the variation  $\beta$  of the Coriolis parameter with latitude is assumed constant. It was shown that the possible modes of oscillation may be described, in that approximation, as a carrier wave, moving always towards the west, modulated by an envelope fixed in space. On this basis the period and general character of the oscillation can be determined quite simply.

The purpose of the present paper is to describe an exact computation of the non-divergent oscillations in a particular type of ocean basin, and to see how far the exact results are in agreement with the  $\beta$ -plane approximation. If the agreement is satisfactory it may then be possible to use the  $\beta$ -plane approximation with confidence in situations where the exact solution would be difficult to obtain. Some preliminary results of this work were mentioned in an earlier paper (Longuet-Higgins 1964 *a*).

The problem to be considered is as follows. Imagine a hemispherical shell of fluid whose boundary is a great-circle passing through the pole of rotation, so that the centre of the shell lies on the equator. The depth of water (i.e. the thickness of the shell) is assumed constant, and is small compared to the radius of the sphere. We seek the free modes of oscillation in such a fluid shell. The amplitude of the oscillations is assumed small enough that the equations may be linearized. The vertical density stratification, though slight, is assumed sufficient to inhibit the vertical component of the Coriolis force.

The problem will be solved by two independent methods. In the first method the pole of coordinates is taken on the axis of rotation, and the solution is expanded in a series of spherical harmonics, as in Goldsbrough (1933). Our situation, however, is simpler than that of Goldsbrough's in that the divergence of the motion is neglected. We thus work in terms of a single function  $\psi$ , the streamfunction.  $\psi$  is expanded in a double series whose terms are products of Legendre polynomials in the colatitude  $\theta$  and of Fourier harmonics in the longitude  $\phi$ . These are selected so as to satisfy the conditions at the boundary. Substitution of this series in the equations of motion gives an infinite set of equations for the coefficients in the series. The solution proceeds by successive approximation, truncating the infinite matrix at successively higher numbers of rows and columns.

In the second method (described in the Appendix) the pole of coordinates is taken not on the axis of rotation but at the central point of the basin, that is to say on the equator. The transformed equation of motion is more complicated, but when the streamfunction is expanded as before the equations for the coefficients are somewhat simpler.

The two methods are found to give results in very close agreement. These results are then compared with the  $\beta$ -plane approximation (see § 8) and the lower modes at least are found to be quite well approximated by the  $\beta$ -plane approximation. Finally, in § 9, the possible application of these results to the Pacific Ocean is discussed.

## 2. FORMULATION OF THE PROBLEM

Take spherical coordinates  $\theta, \phi$  with pole on the axis of rotation; let  $\theta$  denote the colatitude [ $\theta = 0$  at the north pole] and  $\phi$  the longitude. The boundary of the basin may be taken as given by  $\phi = 0$  or  $\phi = \pi$ .

The basin being of uniform depth, the equation to be satisfied by the streamfunction  $\psi$  is

$$\frac{\partial}{\partial t}(\nabla^2\psi) + 2\Omega \frac{\partial\psi}{\partial\phi} = 0, \quad (1)$$

where  $\nabla^2$  denotes the surface Laplacian†

$$\nabla^2 \equiv \frac{1}{\sin\theta} \frac{\partial}{\partial\theta} \left( \sin\theta \frac{\partial}{\partial\theta} \right) + \frac{1}{\sin^2\theta} \frac{\partial^2}{\partial\phi^2},$$

and  $\Omega$  denotes the angular rotation of the globe [cf. § 2 of (I)]. The differential equation (1) is to be solved subject to the boundary condition

$$\psi = 0 \quad \text{when} \quad \phi = 0, \pi. \quad (2)$$

We seek in the first place solutions of (1) which are simple-harmonic in the time  $t$ , with period  $2\pi/\sigma$ .

## 3. FIRST METHOD OF SOLUTION

Let us assume for  $\psi$  the series

$$\psi = \sum_{n=1}^{\infty} \sum_{m=1}^n A_n^m P_n^m(\cos\theta) \sin m\phi e^{-i\sigma t}, \quad (3)$$

where the  $A_n^m$  are constants, complex in general, and  $P_n^m(\mu)$  denotes the associated Legendre polynomial:

$$P_n^m(\mu) = \frac{(1-\mu^2)^{\frac{1}{2}m}}{2^n n!} \frac{d^{n+m}}{d\mu^{n+m}} (\mu^2-1)^n.$$

In (3) it is understood that the real part of the right-hand side is to be taken. Since  $\sin m\phi$  vanishes when  $\phi = 0$  or  $\pi$ , each term of (3) satisfies the required boundary condition, and so, if the series is uniformly convergent, does its sum. Now let us substitute in (1) and assume term-by-term differentiability. Since  $P_n^m(\cos\theta) \sin m\phi$  is a surface harmonic  $S_n(\theta, \phi)$  of degree  $n$  satisfying

$$\nabla^2 S_n + n(n+1) S_n = 0,$$

we have  $i\sigma \sum_{n=1}^{\infty} \sum_{m=1}^n n(n+1) A_n^m P_n^m(\cos\theta) \sin m\phi + 2\Omega \sum_{s=1}^{\infty} \sum_{r=1}^{\infty} r A_s^r P_s^r(\cos\theta) \cos r\phi = 0$ , (4)

to be satisfied when  $0 < \theta < \pi$  and  $0 < \phi < \pi$ . Now in the interval  $0 < \phi < \pi$ , the function  $\cos r\phi$  can be expanded in the sine series:

$$\cos r\phi = \frac{4}{\pi} \sum_{m=1}^{\infty} \frac{m\eta(m,r)}{m^2-r^2} \sin m\phi \quad (0 < \phi < \pi), \quad (5)$$

where

$$\eta(m,r) = \begin{cases} 1 & (m+r) \text{ odd} \\ 0 & (m+r) \text{ even.} \end{cases} \quad (6)$$

† The radius of the globe is taken as unity.

Similarly, let us suppose that, for any given value of  $m$ ,  $P_r^s(\mu)$  can be expanded in the form

$$P_r^s(\mu) = \sum_{n=m}^{\infty} \gamma \begin{pmatrix} r & m \\ s & n \end{pmatrix} P_n^m(\mu) \quad (7)$$

(cf. MacRobert 1926). Then on multiplying each side by  $P_l^m(\mu)$  and integrating term-by-term we have

$$\int_{-1}^1 P_r^s P_l^m d\mu = \gamma \begin{pmatrix} r & m \\ s & l \end{pmatrix} \frac{(l+m)!}{(l-m)!} \frac{1}{l+\frac{1}{2}}, \quad (8)$$

since

$$\int_{-1}^1 P_n^m P_l^m d\mu = \begin{cases} 0 & (l \neq n) \\ \frac{(l+m)!}{(l-m)!} \frac{1}{l+\frac{1}{2}} & (l = n) \end{cases} \quad (9)$$

(see, for example, Whittaker & Watson 1927, §15.51). Writing  $n$  for  $l$  in (8) we have

$$\gamma \begin{pmatrix} r & m \\ s & n \end{pmatrix} = \frac{(n-m)!}{(n+m)!} (n+\frac{1}{2}) I \begin{pmatrix} r & m \\ s & n \end{pmatrix},$$

where  $I \begin{pmatrix} r & m \\ s & n \end{pmatrix}$  denotes the symmetric expression

$$I \begin{pmatrix} r & m \\ s & n \end{pmatrix} = \int_{-1}^1 P_s^r P_n^m d\mu = I \begin{pmatrix} m & r \\ n & s \end{pmatrix}. \quad (10)$$

Substituting the expansions (5) and (7) into the second summation of (4) we have

$$i\sigma \sum_{n=1}^{\infty} \sum_{m=1}^n n(n+1) A_n^m P_n^m(\cos \theta) \sin m\phi + \frac{8\Omega}{\pi} \sum_{s=1}^{\infty} \sum_{r=1}^s r A_s^r \sum_{n=m}^{\infty} \sum_{m=1}^n \frac{(n-m)!}{(n+m)!} (n+\frac{1}{2}) I \begin{pmatrix} r & m \\ s & n \end{pmatrix} \frac{m\eta(m,r)}{m^2-r^2} P_n^m(\cos \theta) \sin m\phi = 0. \quad (11)$$

If we define  $P_n^m(\mu) \equiv 0$  when  $m > n$ , then we have also  $I \begin{pmatrix} r & m \\ s & n \end{pmatrix} = 0$  when  $m > n$ . Hence in the second summation above we have symbolically

$$\sum_{n=m}^{\infty} \sum_{m=1}^n = \sum_{n=1}^{\infty} \sum_{m=1}^n.$$

Then equating coefficients of  $P_n^m(\cos \theta) \sin m\phi$  in (11) we have

$$i\sigma n(n+1) A_n^m + \frac{8\Omega}{\pi} \frac{(n-m)!}{(n+m)!} (n+\frac{1}{2}) \sum_{s=1}^{\infty} \sum_{r=1}^s \frac{mr\eta(m,r)}{m^2-r^2} I \begin{pmatrix} r & m \\ s & n \end{pmatrix} A_s^r = 0, \quad (12)$$

where  $1 \leq m \leq n < \infty$ . For convenience let us write

$$\pi\sigma/8\Omega = \lambda \quad (13)$$

and

$$\left[ \frac{(n+m)!}{(n-m)!} \frac{n(n+1)}{n+\frac{1}{2}} \right]^{\frac{1}{2}} A_n^m = B_n^m. \quad (14)$$

Then the above equation becomes

$$i\lambda B_n^m + \sum_{s=1}^{\infty} \sum_{r=1}^{\infty} Q \begin{pmatrix} m & r \\ n & s \end{pmatrix} B_s^r = 0, \quad (15)$$

where now

$$Q \begin{pmatrix} m & r \\ n & s \end{pmatrix} = \left[ \frac{(n-m)!}{(n+m)!} \frac{n+\frac{1}{2}}{n(n+1)} \frac{(s-r)!}{(s+r)!} \frac{s+\frac{1}{2}}{s(s+1)} \right]^{\frac{1}{2}} \frac{mr}{m^2-r^2} \eta(m, r) I \begin{pmatrix} m & r \\ n & s \end{pmatrix}. \quad (16)$$

Since  $\eta(m, r)$  and  $I \begin{pmatrix} m & r \\ n & s \end{pmatrix}$  are both symmetric in the pairs  $\begin{pmatrix} m \\ n \end{pmatrix}$ ,  $\begin{pmatrix} r \\ s \end{pmatrix}$ , it is evident that  $Q \begin{pmatrix} m & r \\ n & s \end{pmatrix}$  is *antisymmetric* in  $\begin{pmatrix} m \\ n \end{pmatrix}$ ,  $\begin{pmatrix} r \\ s \end{pmatrix}$ , i.e. if  $\begin{pmatrix} m \\ n \end{pmatrix}$  is interchanged with  $\begin{pmatrix} r \\ s \end{pmatrix}$  the sign of  $Q$  is reversed. It is convenient to regard the summation with respect to  $r, s$  in (15) as a simple summation over all allowable values of  $r, s$ . (These can of course be placed in a single ordered sequence.) Hence we can write

$$\lambda B_n^m = \sum_{\begin{pmatrix} r \\ s \end{pmatrix}} iQ \begin{pmatrix} m & r \\ n & s \end{pmatrix} B_s^r, \quad (17)$$

so that  $\lambda$  is an eigenvalue of the Hermitian matrix  $iQ$  and is therefore real. Each eigenvalue  $\lambda$  and the corresponding eigenvector  $B_n^m$  corresponds to a free mode of oscillation; the period of the oscillation in days is given by

$$\frac{\Omega}{\sigma} = \frac{\pi}{8\lambda} = \frac{0.3927}{\lambda} \quad (18)$$

and the corresponding constants in the series (3) are given by

$$A_n^m = \left[ \frac{(n-m)!}{(n+m)!} \frac{n+\frac{1}{2}}{n(n+1)} \right]^{\frac{1}{2}} B_n^m. \quad (19)$$

#### 4. NATURE OF THE SOLUTIONS

A closer inspection of the matrix  $Q$  will show more clearly the character of the solutions. In equation (10),  $P_n^m$  is an odd or even function of  $\mu$  according as  $(n-m)$  is odd or even; and similarly for  $P_s^r$ . Hence we see that  $I \begin{pmatrix} m & r \\ n & s \end{pmatrix}$  vanishes unless  $(n-m)$  and  $(s-r)$  are both even or both odd. On the other hand  $\eta(m, r)$ , by (6), vanishes unless  $m$  and  $r$  are of different parity. Since  $I \begin{pmatrix} m & r \\ n & s \end{pmatrix}$  and  $\eta(m, r)$  are both factors of  $Q \begin{pmatrix} m & r \\ n & s \end{pmatrix}$  we have the following possibilities for non-zero  $Q$ :

$$\begin{pmatrix} m & r \\ n & s \end{pmatrix} = \begin{pmatrix} \text{odd} & \text{even} \\ \text{odd} & \text{even} \end{pmatrix} \quad \text{or} \quad \begin{pmatrix} \text{even} & \text{odd} \\ \text{even} & \text{odd} \end{pmatrix}, \quad (20)$$

$$\begin{pmatrix} m & r \\ n & s \end{pmatrix} = \begin{pmatrix} \text{odd} & \text{even} \\ \text{even} & \text{odd} \end{pmatrix} \quad \text{or} \quad \begin{pmatrix} \text{even} & \text{odd} \\ \text{odd} & \text{even} \end{pmatrix}. \quad (21)$$

In (17), if  $\begin{pmatrix} m \\ n \end{pmatrix} = \begin{pmatrix} \text{odd} \\ \text{odd} \end{pmatrix}$ , then the summation can be taken over  $\begin{pmatrix} r \\ s \end{pmatrix} = \begin{pmatrix} \text{even} \\ \text{even} \end{pmatrix}$ , and vice versa. So we have

$$\lambda \begin{matrix} B_n^m \\ \text{(odd)} \\ \text{(odd)} \end{matrix} = \sum_{\begin{matrix} \text{(r)} \\ \text{(s)} = \text{(even)} \\ \text{(even)} \end{matrix}} iQ \begin{pmatrix} m & r \\ n & s \end{pmatrix} B_s^r, \quad (22)$$

and similarly

$$\lambda \begin{matrix} B_s^r \\ \text{(even)} \\ \text{(even)} \end{matrix} = \sum_{\begin{matrix} \text{(m')} \\ \text{(n')} = \text{(odd)} \\ \text{(odd)} \end{matrix}} iQ \begin{pmatrix} r & m' \\ s & n' \end{pmatrix} B_n^{m'}. \quad (23)$$

Hence substituting for  $B_s^r$  in (20) we have

$$\lambda^2 B_n^m = R \begin{pmatrix} m & m' \\ n & n' \end{pmatrix} B_n^{m'}, \quad (24)$$

where  $\begin{pmatrix} m \\ n \end{pmatrix}$  is  $\begin{pmatrix} \text{odd} \\ \text{odd} \end{pmatrix}$  and

$$R \begin{pmatrix} m & m' \\ n & n' \end{pmatrix} = - \sum_{\substack{(r) = (\text{even}) \\ (s) = (\text{even})}} Q \begin{pmatrix} m & r \\ n & s \end{pmatrix} Q \begin{pmatrix} r & m' \\ s & n' \end{pmatrix}. \quad (25)$$

But  $Q$  is antisymmetric in  $\begin{pmatrix} m & r \\ n & s \end{pmatrix}$  and so

$$R \begin{pmatrix} m & m' \\ n & n' \end{pmatrix} = \sum_{\substack{(r) = (\text{even}) \\ (s) = (\text{even})}} Q \begin{pmatrix} m & r \\ n & s \end{pmatrix} Q \begin{pmatrix} m' & r \\ n' & s \end{pmatrix}, \quad (26)$$

a real symmetric matrix. In practice we can solve the eigenvalue equation (22) for  $\lambda^2$  and  $B_n^m$  and then find  $B_s^r$  from (21).

Since  $Q$  is real, equations (20) and (21) show that if  $B_n^m$  is real, then  $B_s^r$  is imaginary, and similarly for  $A_n^m$  and  $A_s^r$ . So the solution (3) can then be written

$$\psi = \psi_1 \cos \sigma t + \psi_2 \sin \sigma t,$$

where

$$\left. \begin{aligned} \psi_1 &= \sum_{\substack{(m) = (\text{odd}) \\ (n) = (\text{odd})}} A_n^m P_n^m(\cos \theta) \sin m\phi, \\ \psi_2 &= \sum_{\substack{(r) = (\text{even}) \\ (s) = (\text{even})}} (-i) A_s^r P_s^r(\cos \theta) \sin s\phi, \end{aligned} \right\}$$

and  $\psi_1, \psi_2$  represent the in-phase and quadrature components of the motion. We may also define an ‘amplitude’

$$a = (\psi_1^2 + \psi_2^2)^{\frac{1}{2}}$$

and phase

$$\chi = \tan^{-1}(\psi_2/\psi_1)$$

in terms of which

$$\psi = a \cos(\sigma t - \chi).$$

Since in the case just treated  $(n-m)$  and  $(s-r)$  are both even, it follows that  $\psi$  is an even function of  $\cos \theta$  and so symmetric about the equator. We call such solutions ‘symmetric modes’. If, however, starting from (21) instead of (20) we assume  $\begin{pmatrix} m \\ n \end{pmatrix} = \begin{pmatrix} \text{odd} \\ \text{even} \end{pmatrix}$  and  $\begin{pmatrix} r \\ s \end{pmatrix} = \begin{pmatrix} \text{even} \\ \text{odd} \end{pmatrix}$  we obtain, by exactly similar steps, the ‘antisymmetric modes’. These are modes in which  $\psi$  is an odd function of  $\cos \theta$ , and so the equator is always a streamline.

## 5. METHOD OF COMPUTATION

The analytical properties of the integral  $I \begin{pmatrix} m & r \\ n & s \end{pmatrix}$  defined by equation (10) seem to have been elucidated only in certain special cases, as when  $r = m$  (see equation (9)). It can be shown (see Longuet-Higgins & Crease, MS. in preparation) that  $I \begin{pmatrix} m & r \\ n & s \end{pmatrix}$  generally satisfies certain three-term recurrence relations and that it is in fact the sum of a  ${}_4F_3$ , that is, a

generalized hypergeometric series.† The series can be transformed in various ways so as always to have only a finite number of terms.

For the purpose of computation, however,  $I \begin{pmatrix} m & r \\ n & s \end{pmatrix}$  was evaluated in two independent ways: first directly by quadratures; and secondly by substituting in (10) the series

$$P_n^m(\mu) = \frac{(2n)!}{2^{2n}n!} (1-\mu^2)^{\frac{1}{2}m} \left[ \frac{\mu^{n-m}}{(n-m)!} - \frac{1}{2(2n-1)} \frac{\mu^{n-m-2}}{(n-m-2)!} + \frac{1}{2 \cdot 4 \cdot (2n-1)(2n-3)} \frac{\mu^{n-m-4}}{(n-m-4)!} - \dots \right].$$

On multiplying by the corresponding expression for  $P_s^r(\mu)$  and integrating term-by-term, using

$$\int_{-1}^1 (1-\mu^2)^p \mu^{2q} d\mu = \frac{p!(q-\frac{1}{2})!}{(p+q+\frac{1}{2})!},$$

we easily obtain  $I \begin{pmatrix} m & r \\ n & s \end{pmatrix}$  in the form of a finite double series:

$$I \begin{pmatrix} m & r \\ n & s \end{pmatrix} = \frac{2^{n+s}}{\pi} \sum_{i=0}^{[\frac{1}{2}(n-m)]} \sum_{j=0}^{[\frac{1}{2}(s-r)]} \left(-\frac{1}{4}\right)^{i+j} \frac{(n-i-\frac{1}{2})!(s-j-\frac{1}{2})!}{i!j!(n-m-2i)!(s-r-2j)!} \times \frac{\{\frac{1}{2}(n-m+s-r-1)-(i+j)\}!\{\frac{1}{2}(m+r)\}!}{\{\frac{1}{2}(n+s+1)-(i+j)\}!}.$$

The two methods gave results in agreement up to at least five significant figures (for  $m \leq n \leq 10$ ,  $r \leq s \leq 10$ ). The double summation method was then checked against the sum of the generalized hypergeometric series and was found to be in agreement to at least eight significant figures. The double series method was that eventually used.

The calculation of the eigenfunctions from equations (17) and (24) was carried out by truncating the matrix  $Q \begin{pmatrix} m & r \\ n & s \end{pmatrix}$  at successively higher numbers of rows and columns. Thus it was supposed that (for the symmetric modes)

$$m \leq n \leq 2k-1, \quad r \leq s \leq 2k,$$

where  $k$  was taken successively to be 1, 2, 3 ... 8; and for the antisymmetric modes

$$m < n \leq 2k, \quad r < s \leq 2k+1,$$

with the same sequence of values for  $k$ . Each series for  $\psi_1$  and  $\psi_2$  then contained  $\frac{1}{2}k(k+1)$  terms; hence the matrices  $Q$  and  $R$  contained also  $\frac{1}{2}k(k+1)$  rows and columns. The eigenvalues and eigenvectors of  $R$  were extracted by a standard routine‡, capable of handling matrices of high order. These and the subsequent computations were carried out on an I.B.M. 7090 digital computer.

The results of these computations are set out in the next two sections. It should be mentioned that the numerical results were checked by a completely independent method, which is described in the appendix. All the results quoted were verified to at least six significant figures.

† See also Ashour (1964).

‡ Subroutine NU-MLEW; SHARE Program no. 1588. This subroutine uses Householder's (1958) method to reduce the matrix to tridiagonal form; Givens's (1954) method of finding the eigenvalues, and Wilkinson's (1958) method of calculating the corresponding eigenvectors.



## 6. THE EIGENVALUES

When  $k = 1$  (the lowest approximation) both methods of approximation yield the single eigenvalue

$$\frac{\sigma}{\Omega} = \frac{\sqrt{15}}{8} = 0.484123$$

for the symmetric mode and

$$\frac{\sigma}{\Omega} = \frac{5}{48}\sqrt{7} = 0.194878$$

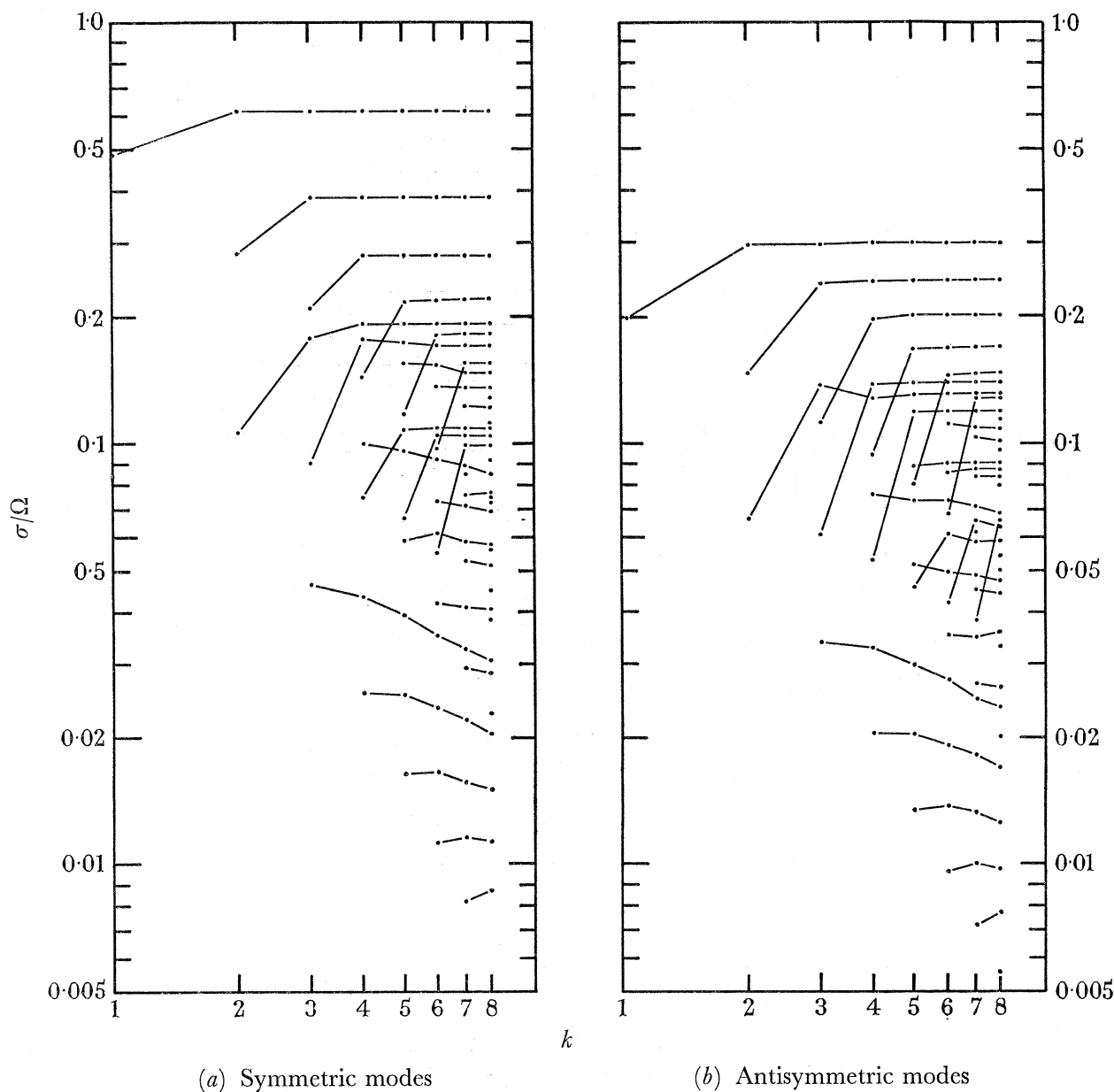


FIGURE 1. Convergence diagram for the eigenvalues.  $\sigma/\Omega$  denotes the frequency;  $k$  denotes the degree of the approximation.

for the antisymmetric mode. At the  $k$ th approximation, involving the resolution of a matrix of  $\frac{1}{2}k(k+1)$  rows and columns, one obtains  $\frac{1}{2}k(k+1)$  eigenvalues. These were calculated up to  $k = 8$  and are shown graphically in figure 1.

## PLANETARY WAVES ON A HEMISPHERE

325

Figure 1 illustrates roughly the rate of convergence. Corresponding eigenvalues have been connected by a broken line, the succession being determined by examination of the corresponding eigenvectors.

For example, the mode corresponding to the largest eigenvalue is dominated by the term in  $P_2^2(\cos\theta)$  (in the in-phase component  $\psi_1$ ). The quadrature component  $\psi_2$  contains (eventually) large coefficients of both  $P_1^1$  and  $P_3^3$ . However,  $P_3^3$  can occur first only in the second approximation ( $k = 2$ ). Thus we see why the eigenfrequency for  $k = 1$  lies not very close to the eigenfrequencies of the corresponding mode when  $k \geq 2$ .

Similar considerations apply to the other modes: no eigenfrequency can be well established until the corresponding approximation includes all the main spherical harmonics in that mode.

In general, convergence is most rapid for the largest eigenvalues. When  $k = 8$  those eigenvalues less than about 0.01 are not yet well established.

TABLE 1. SUCCESSIVE APPROXIMATIONS TO THE FREQUENCY  $\sigma/\Omega$  OF THE THREE LOWEST SYMMETRIC MODES ( $\Delta$  DENOTES THE FIRST DIFFERENCE)

$k$	mode 1		mode 2		mode 3	
	$\sigma/\Omega$	$\Delta$	$\sigma/\Omega$	$\Delta$	$\sigma/\Omega$	$\Delta$
1	0.484 123	—	—	—	—	—
2	0.610 577	—	0.285 391	—	—	—
3	0.614 081	3504	0.379 587	—	0.209 117	—
4	0.614 977	896	0.382 409	2822	0.275 633	—
5	0.615 313	336	0.383 293	784	0.277 734	2101
6	0.615 468	155	0.383 670	377	0.278 479	745
7	0.615 550	082	0.383 860	190	0.278 824	345
8	0.615 596	046	0.383 966	106	0.279 008	184

The rate of convergence of successive approximations is illustrated numerically in table 1, from which it can be seen that the convergence is indeed rapid; the difference between successive approximations decreases nearly exponentially as  $k$  increases. From this property one can estimate the order of the error in the calculated frequency. However, the procedure is clearly valid only for those modes whose frequencies are already well established.

The frequencies of all such modes, as given by the approximation  $k = 8$ , are listed in the first column of table 2, the estimated error being possibly one unit in the last decimal place.

TABLE 2A. FREQUENCIES AND PERIODS OF THE WELL-ESTABLISHED SYMMETRIC MODES

	frequency in c/day	period in days	largest coefficient	$\frac{n(n+1)}{2m}$
(1)	0.6156	1.624	$B_2^2$	1.5
	0.384	2.60	$B_4^4$	2.5
	0.279	3.58	$B_6^6$	3.5
	0.219	4.56	$B_8^8$	4.5
	0.181	5.5	$B_{10}^{10}$	5.5
(2)	0.192	5.22	$B_5^3$	5.0
	0.170	5.88	$B_7^5$	5.6
	0.148	6.75	$B_9^7$	6.43...
	0.137	7.3	$B_{11}^9$	7.33...
(3)	0.109	9.1	$B_9^5$	9.0
	0.105	9.5	$B_{11}^7$	9.43...

TABLE 2B. FREQUENCIES AND PERIODS OF THE WELL-ESTABLISHED ANTISYMMETRIC MODES

	frequency in c/day	period in days	largest coefficients	$\frac{n(n+1)}{2m}$
(1)	0.300	3.333	$B_3^2, B_4^3$	3.0, 3.33 ...
	0.243	4.11	$B_5^4, B_6^5$	3.75, 4.2
	0.201	4.99	$B_7^6, B_8^7$	4.67 ..., 5.14 ...
	0.170	5.89	$B_9^8, B_{10}^9$	5.625, 6.11 ...
	0.147	6.80	$B_{11}^{10}, B_{12}^{11}$	6.6, 7.08 ...
(2)	0.140	7.15	$B_7^4$	7.0
	0.131	7.66	$B_9^6$	7.5
	0.119	8.4	$B_{11}^8$	8.25
	0.108	9.3	$B_{13}^{10}$	9.1
(3)	0.090	11.1	$B_{11}^6$	11.0
	0.087	11.5	$B_{13}^8$	11.375

## 7. THE EIGENVECTORS

Table 3 shows the distribution of the normalized coefficients  $B_n^m$  for a typical mode: the symmetric mode with frequency  $\sigma/\Omega = 0.192$ . It can be seen that the largest (in absolute value) of the coefficients is  $B_5^3$ , with a magnitude of 0.8749. The two neighbouring coefficients  $B_4^3$  and  $B_6^3$  are almost as large, but the others decrease rapidly with separation from the main harmonic. (When  $n \geq 10$  the coefficients are not expected to be very accurate.)

TABLE 3. NUMERICAL VALUES OF THE COEFFICIENTS  $B_n^m$  IN  $\psi_1$  AND  $-iB_n^m$  IN  $\psi_2$ , FOR THE SYMMETRIC MODE WITH FREQUENCY  $\sigma/\Omega = 0.192$ 

$n \backslash m$	1	2	3	4	5	6	7	8	9	10	11	12	13	14	15	16
1	-0.0124	—	0.2463	—	-0.0288	—	-0.0077	—	-0.0019	—	-0.0007	—	-0.0003	—	-0.0002	—
2	—	0.0015	—	-0.6227	—	0.0376	—	0.0208	—	-0.0004	—	-0.0006	—	-0.0005	—	-0.0003
3	—	—	-0.0030	—	-0.8749	—	-0.0018	—	-0.0078	—	-0.0041	—	-0.0022	—	-0.0012	—
4	—	—	—	0.0218	—	0.7749	—	0.0342	—	0.0100	—	0.0032	—	0.0011	—	0.0005
5	—	—	—	—	0.0062	—	0.3746	—	0.0164	—	-0.0006	—	-0.0022	—	-0.0018	—
6	—	—	—	—	—	0.0305	—	-0.0222	—	0.0177	—	0.0094	—	0.0046	—	0.0024
7	—	—	—	—	—	—	0.0207	—	0.0851	—	0.0179	—	0.0038	—	0.0003	—
8	—	—	—	—	—	—	—	0.0613	—	-0.0202	—	0.0069	—	0.0063	—	0.0039
9	—	—	—	—	—	—	—	—	0.1404	—	0.0349	—	0.0146	—	0.0055	—
10	—	—	—	—	—	—	—	—	—	-0.1287	—	-0.0152	—	0.0010	—	0.0024
11	—	—	—	—	—	—	—	—	—	—	-0.0427	—	0.0170	—	0.0110	—
12	—	—	—	—	—	—	—	—	—	—	—	-0.0225	—	-0.0117	—	-0.0034
13	—	—	—	—	—	—	—	—	—	—	—	—	-0.0196	—	0.0087	—
14	—	—	—	—	—	—	—	—	—	—	—	—	—	-0.0092	—	-0.0099
15	—	—	—	—	—	—	—	—	—	—	—	—	—	—	-0.0131	—
16	—	—	—	—	—	—	—	—	—	—	—	—	—	—	—	-0.0012

This example was found to be typical of the well-established modes: in each mode there was generally one coefficient  $B_n^m$  which was clearly the greatest. However, in some of the antisymmetric modes (table 2B) the two largest coefficients were found to be of nearly equal magnitude. In such cases both are listed.

One would naturally expect the period of each mode to be approximately equal to the period of the free mode (on the unbounded sphere) corresponding to the dominant harmonics. That is to say we expect

$$\Omega/\sigma \doteq n(n+1)/2m,$$

where  $B_n^m$  is a dominant harmonic. The values of this expression are tabulated in the fourth column of table 2, and it will be seen that there is indeed rough agreement with the more accurate values shown in column 2.

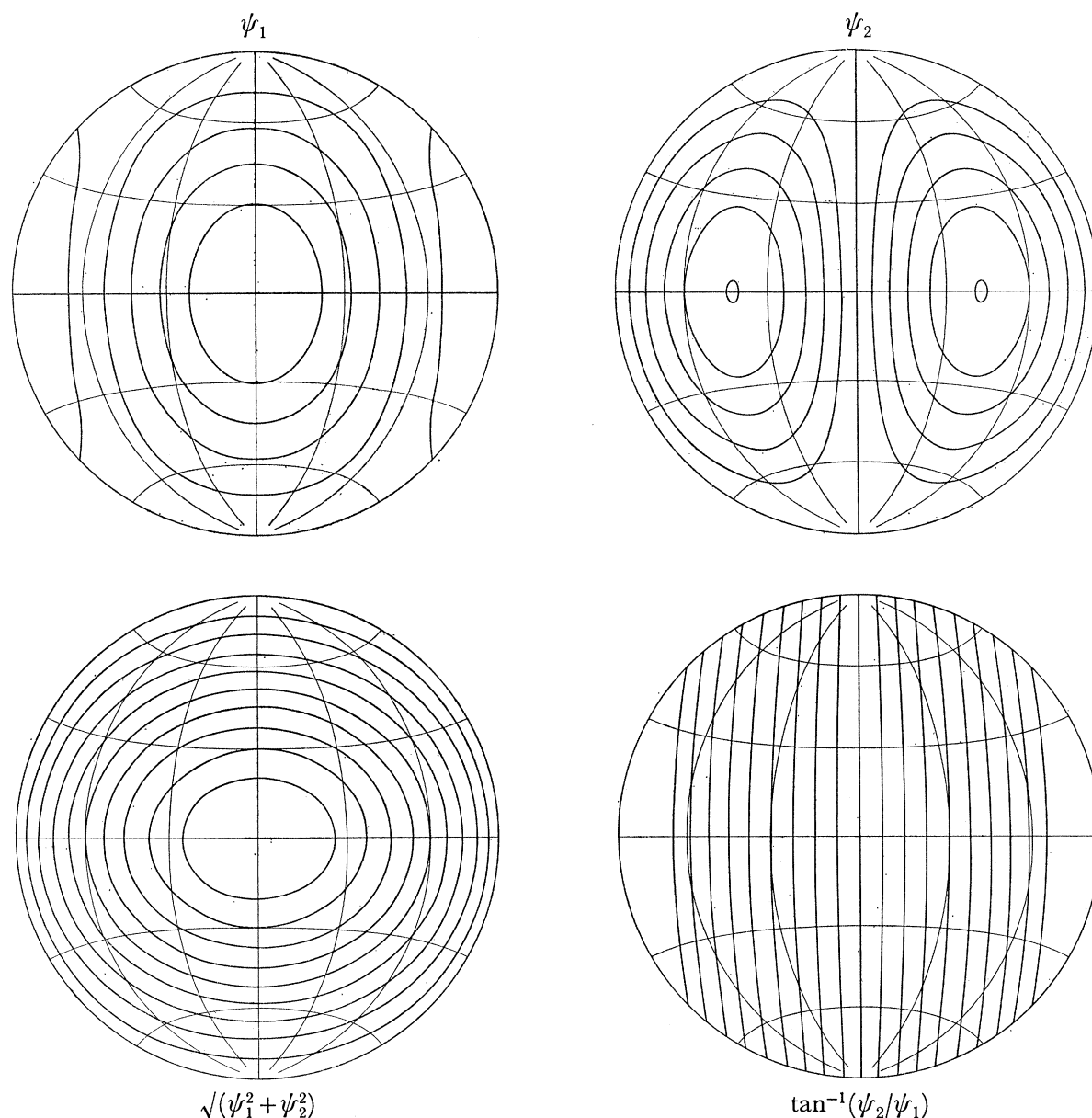


FIGURE 2. The streamfunction for the lowest symmetric mode ( $T = 1.624$ ).  $\psi_1$  denotes the in-phase component,  $\psi_2$  the quadrature component. Below are the corresponding amplitude and phase functions.

### 8. THE STREAMFUNCTIONS

The streamfunctions  $\psi$  are shown in figures 2 to 11. From these it can be seen that the symmetric modes, for example, fall into three groups, according as  $\psi_1$  and  $\psi_2$  have 1, 3 or 5 rows of circulating cells from pole to pole (see figures 2 to 6). The order of the modes within each group corresponds roughly to the number of cells along a circle of latitude. The antisymmetric modes, shown in table 2 B, fall into three similar groups, having respectively

2, 4 and 6 rows of cells from pole to pole (see figures 7 to 11). Whether all the modes of still higher order can be grouped in a similar way remains to be determined.

Consider the streamlines for the lowest symmetric oscillation, shown in figure 2. At time  $t = 0$ , say, the streamlines are given by the in-phase component  $\psi_1$ . It can be seen that the

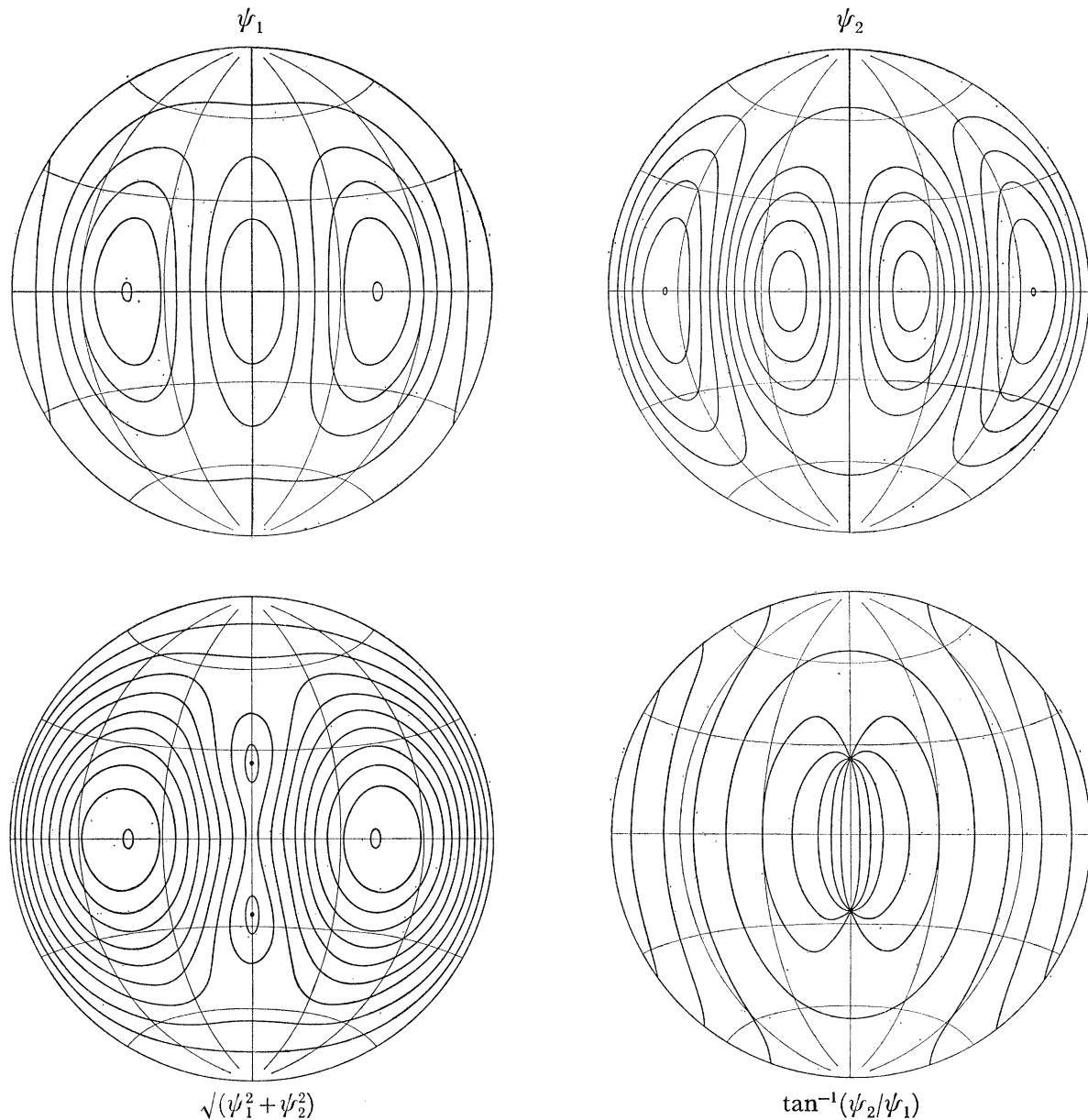


FIGURE 3. The streamfunction for the next lowest symmetric mode ( $T = 2.60$ ), with the amplitude and phase functions.

currents consist of a single circulating cell placed centrally in the basin, but with very weak cells flanking it to either side. The central cell then migrates westwards, and the cell at the eastern edge of the basin becomes stronger and moves westwards. At  $t = \frac{1}{4}T$  (where  $T$  is the period) the streamfunction is equal to  $\psi_2$ . From figure 2 we see that the two cells are now of equal dimensions. At  $t = \frac{1}{2}T$  the first cell has moved to the westwards edge of basin and the second cell has moved to the centre. The streamlines are again as for  $t = 0$  but with the

direction of the circulation reversed. Similarly, at  $t = \frac{3}{4}T$  the streamlines are as for  $t = \frac{1}{4}T$ , but with the direction of the circulation reversed.

Thus the lowest mode consists of a succession of cells, of alternate sign, arising at the eastern boundary of the basin, drifting westwards and vanishing at the western edge.

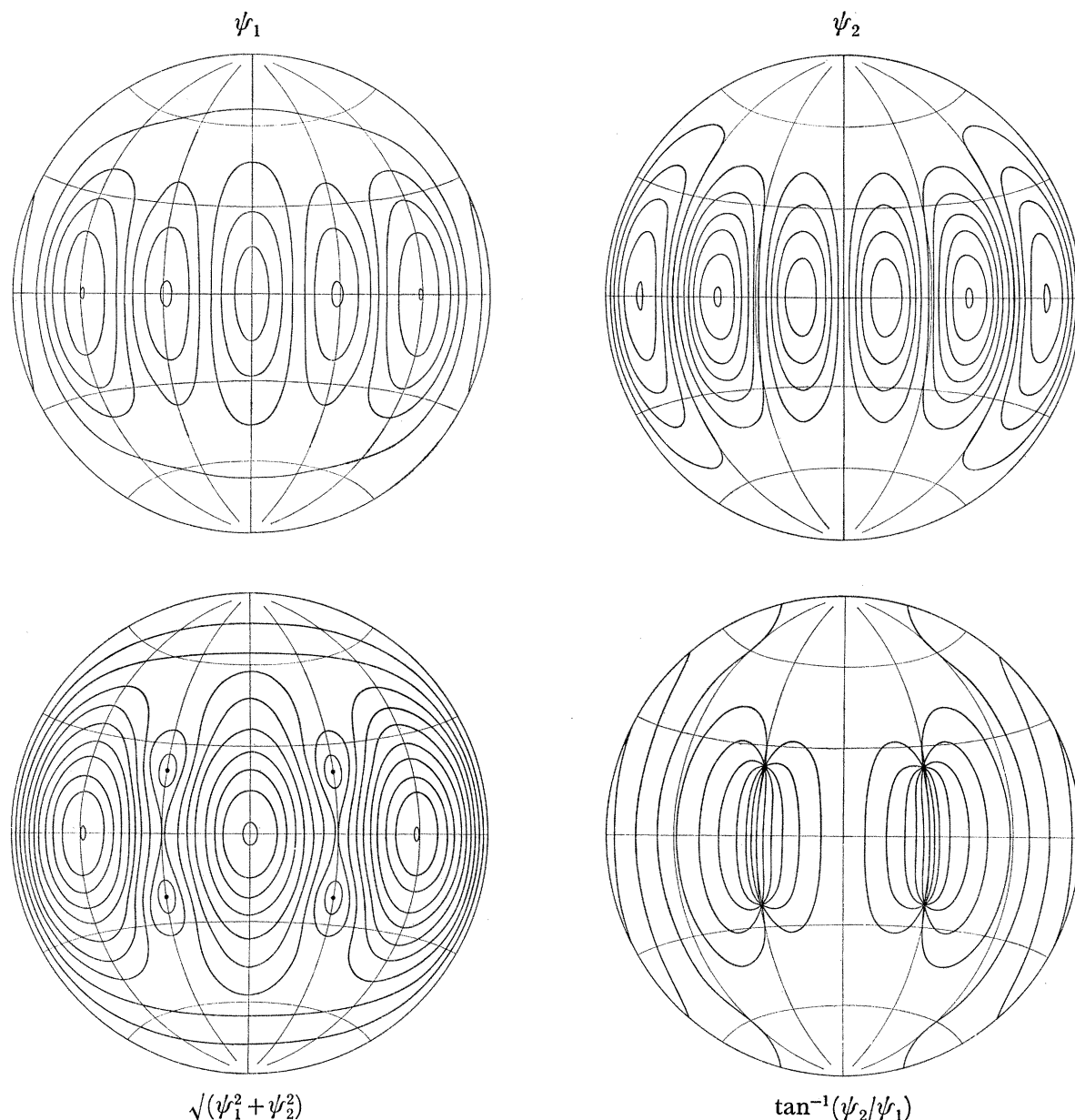
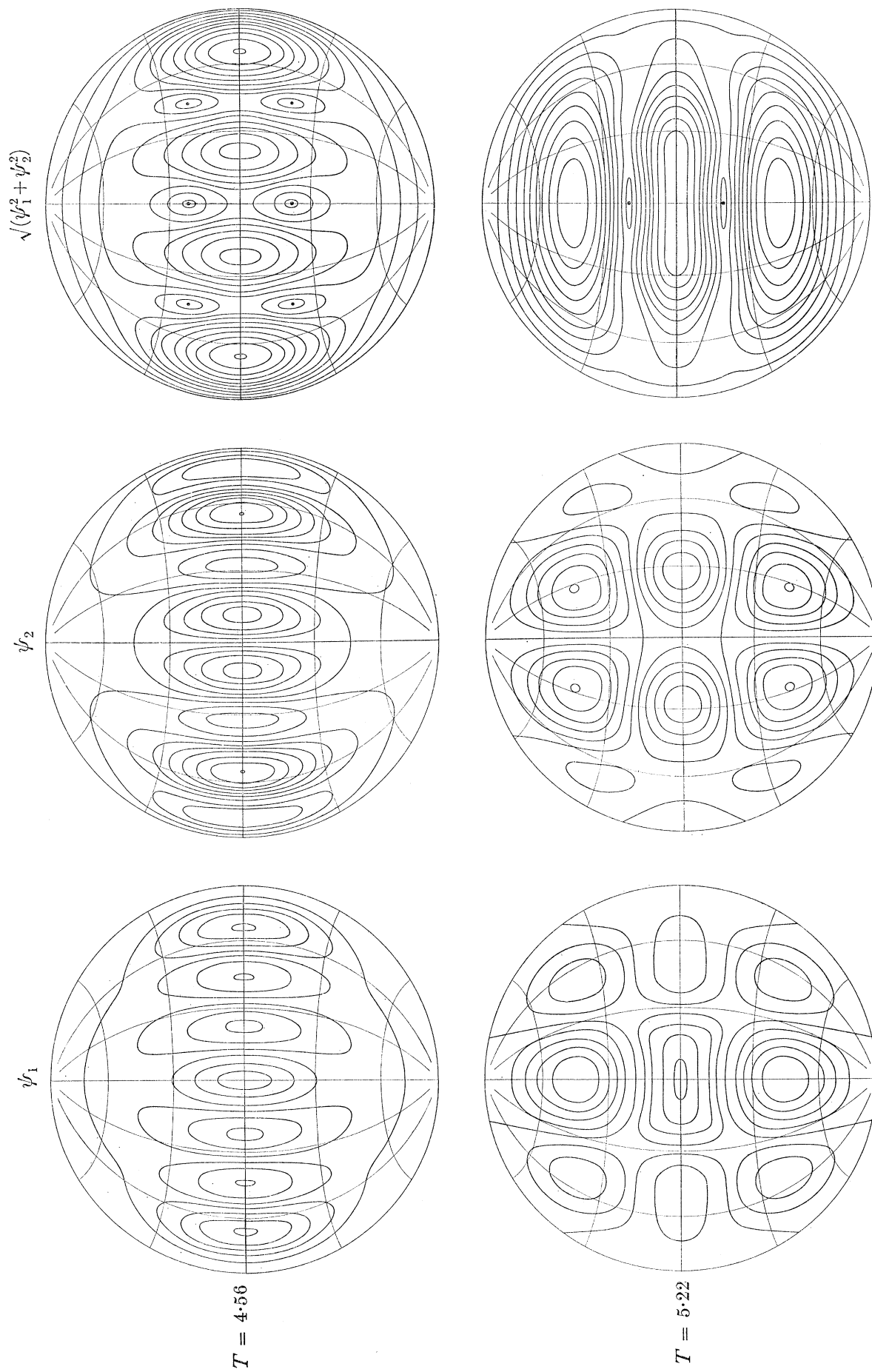


FIGURE 4. The streamfunction for the third symmetric mode ( $T = 3.58$ ), with the amplitude and phase functions.

The higher modes will be found to behave in a similar way.

Let us see how far these modes can be described by the ' $\beta$ -plane approximation'. In this approximation the spherical basin is replaced locally by a plane surface tangent at the centre of the basin, that is to say at a point on the equator. The rate of change  $\beta$  of the



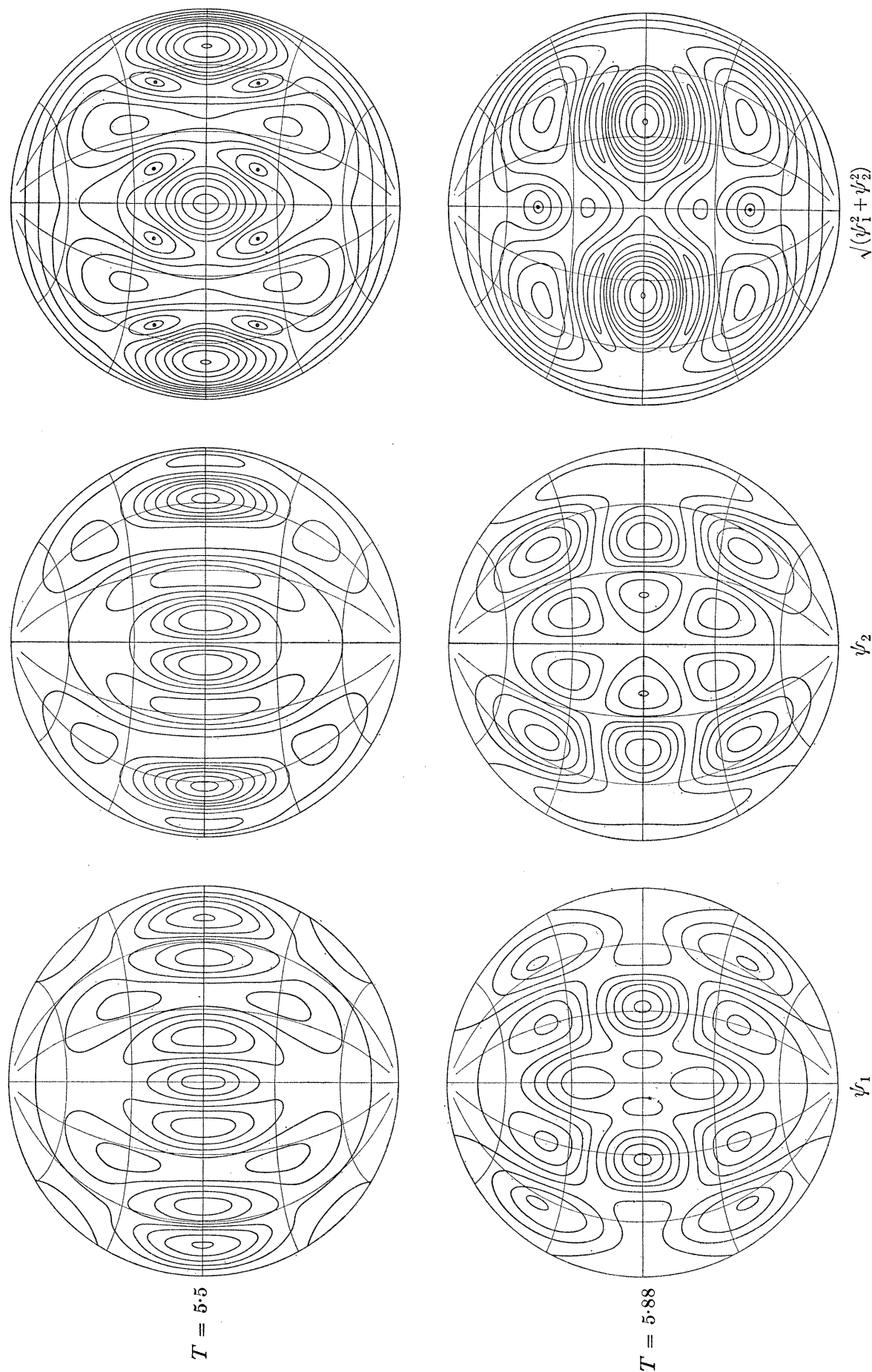
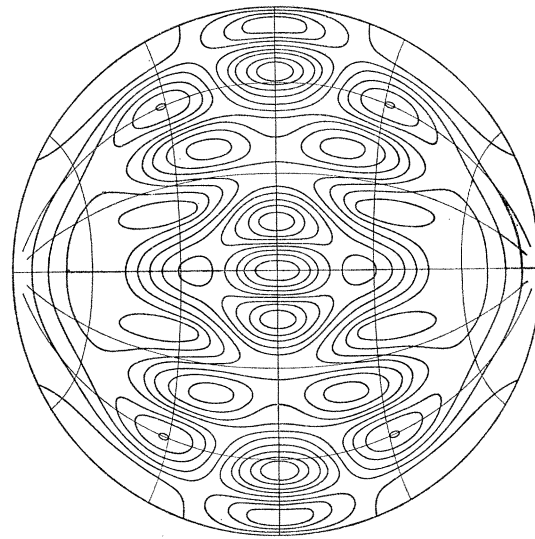
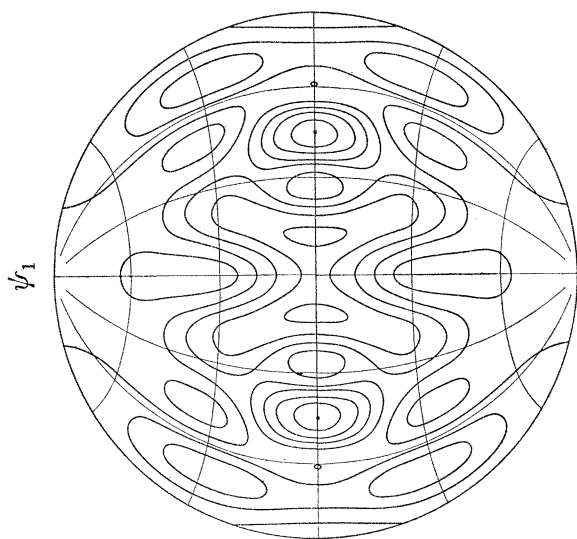
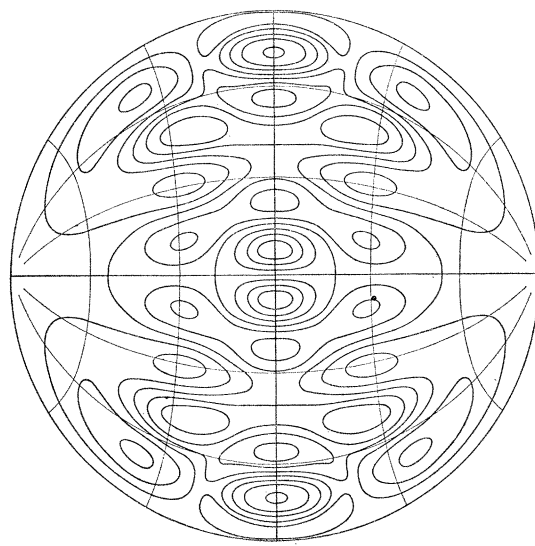
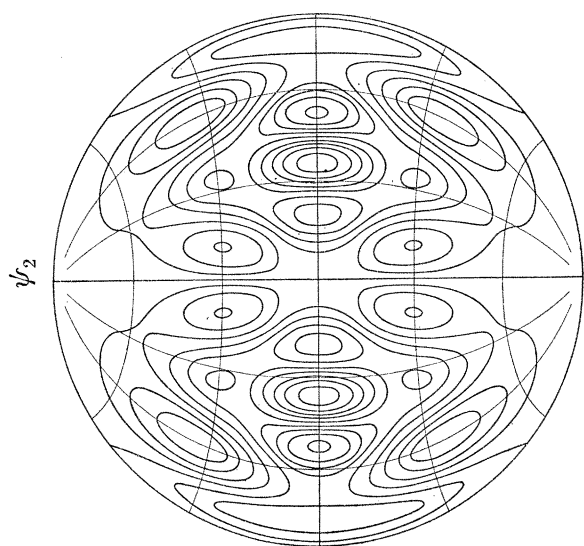


FIGURE 5. Streamlines of higher symmetric modes, with the corresponding amplitude functions.





$T = 6.75$

$T = 7.3$

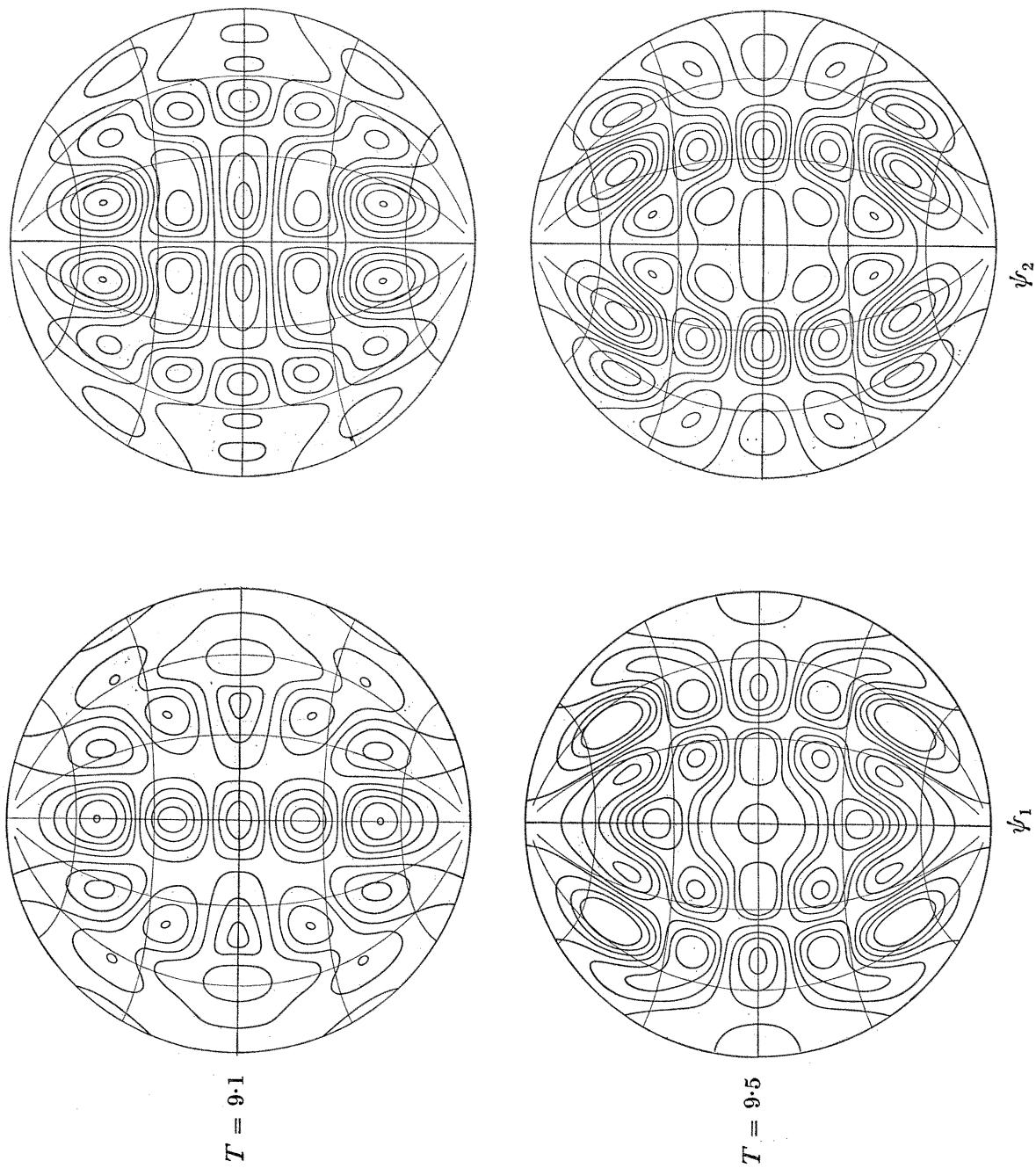


Figure 6. Streamlines of higher symmetric modes.

Coriolis parameter with latitude is assumed to be constant and everywhere equal to its value at the centre of the basin, that is to say

$$\beta = 2\Omega,$$

the radius of the sphere being taken as unity. The boundary of the basin is a circle of radius  $a$ .

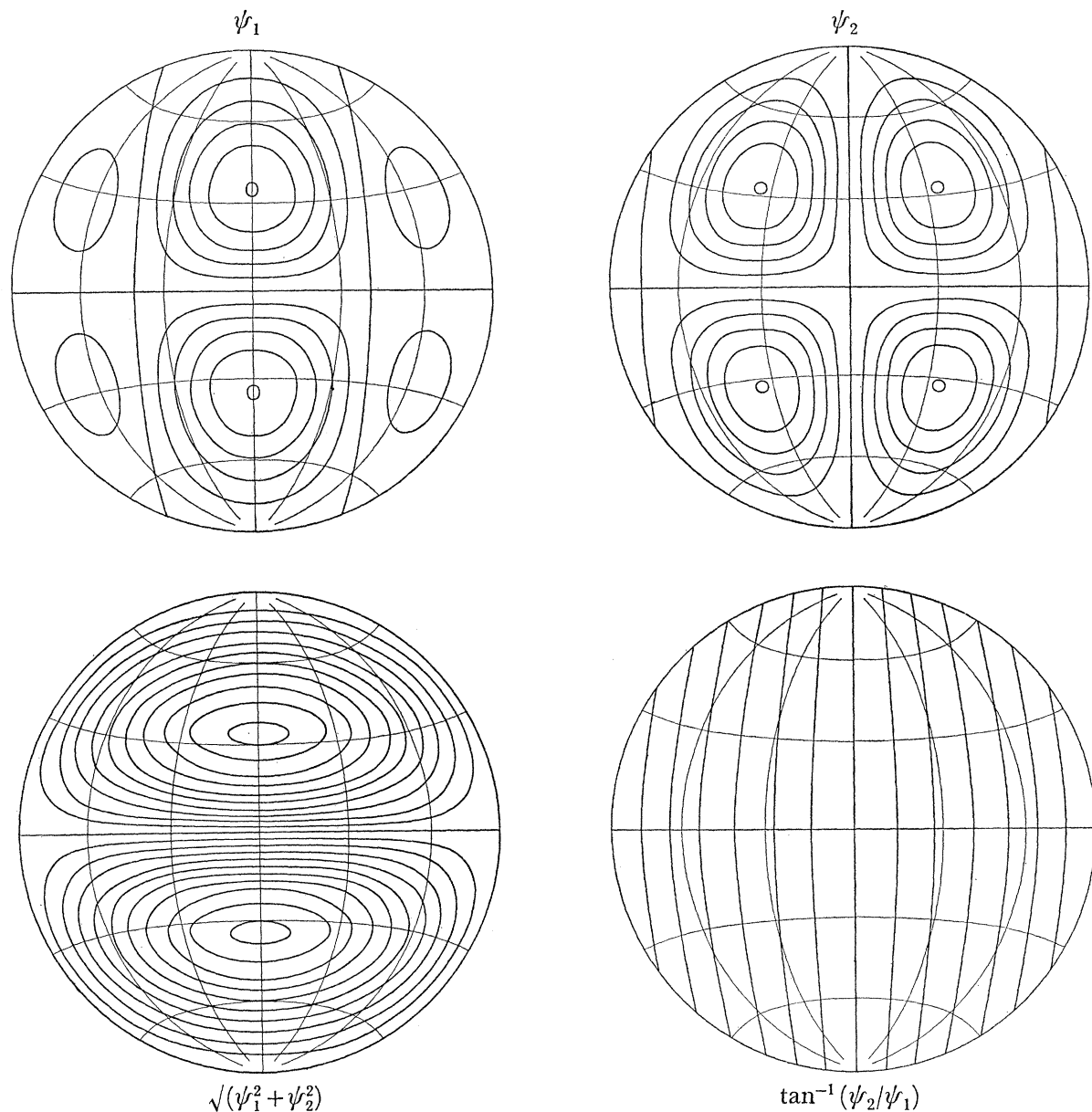


FIGURE 7. The streamfunction for the lowest antisymmetric mode ( $T = 3.333$ ), with the corresponding amplitude and phase functions.

Now the normal-mode solutions for a circular basin on a  $\beta$ -plane have been described in I (§§ 1.9 and 1.10). If  $x$  denotes the eastward coordinate,  $r$  denotes the radial distance from the centre, then the normal mode solutions are given by a stream function of the form

$$\psi = J_n(\gamma r) \frac{\cos}{\sin} \left( n \tan^{-1} \frac{y}{x} \right) \exp[-i(\gamma x + \sigma t)], \quad (25)$$

where  $J_n(z)$  is the Bessel function of integral order  $n$ , and  $\gamma = \Omega/\sigma$ , the period in days. In order that the boundary shall be a streamline we must have

$$\gamma a = z_{n,m} \quad (26)$$

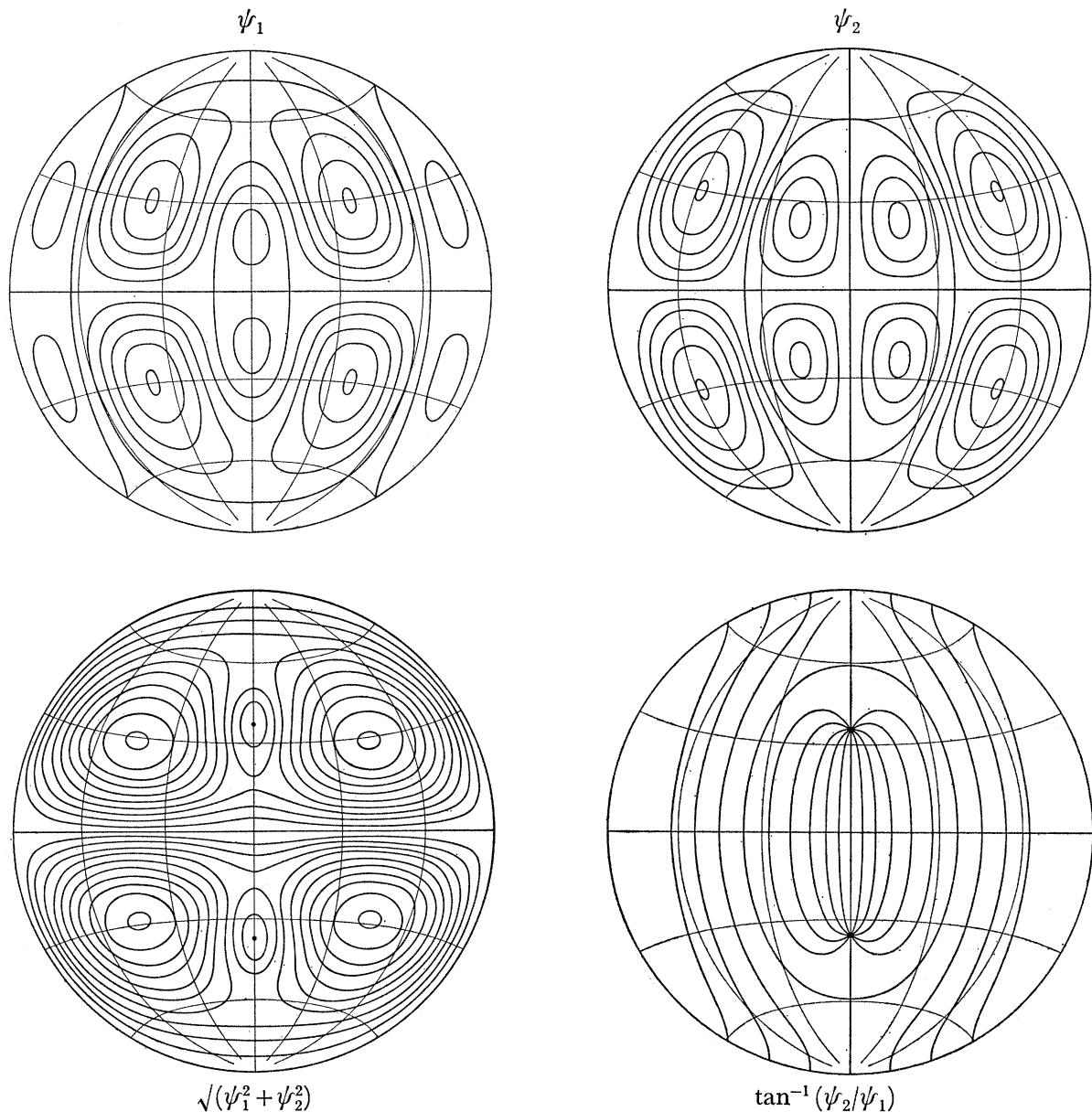


FIGURE 8. The streamfunction for the next lowest antisymmetric mode ( $T = 4.11$ ), with the amplitude and phase functions.

where  $z_{n,m}$  is the  $m$ th zero of  $J_n(z)$ . If we assume that the circle is of radius  $\frac{1}{2}\pi$ , then

$$\gamma = 2z_{n,m}/\pi. \quad (27)$$

The values of  $z_{n,m}$  not exceeding 15 are shown for convenience in table 4.

Equation (25) shows that  $\psi$  can be considered as a carrier wave  $\exp[-i(\gamma x + \sigma t)]$  travelling from east to west (with wavelength  $2\pi/\gamma$  and crests running due north-south) modulated by an envelope function  $J_n(\gamma r) \frac{\cos}{\sin} \{n \tan^{-1}(y/x)\}$ . The envelope function is

identical with that describing the free oscillations of a circular membrane of radius  $a$ , clamped at the boundary. Thus the streamlines  $\psi = 0$  at any fixed instant are of two kinds: the nodal lines of the carrier wave, running in a north–south direction, and the nodal lines of the envelope, which are  $m$  concentric circles and  $n$  straight lines through the origin.

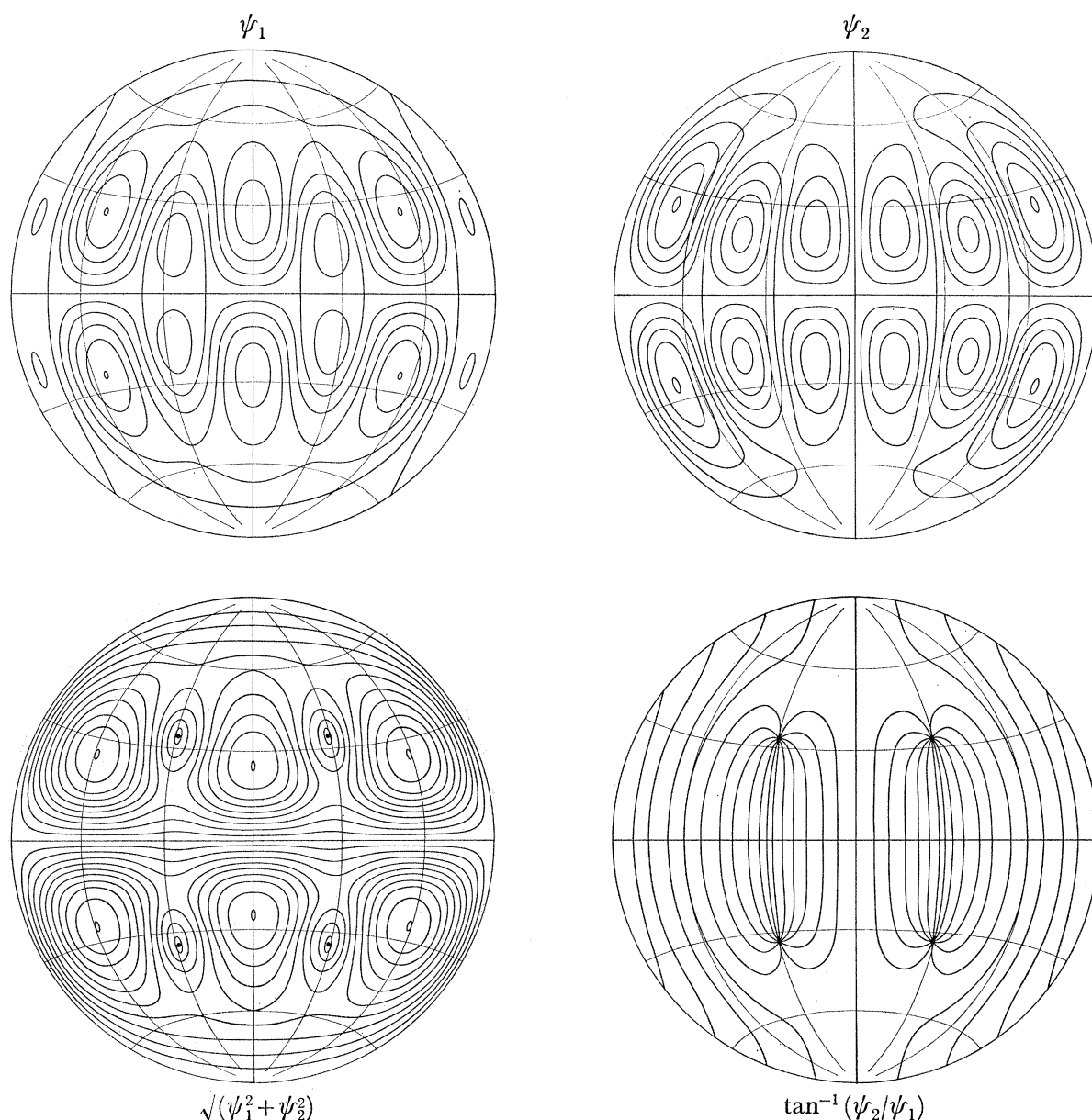


FIGURE 9. The streamfunction for the third antisymmetric mode ( $T = 4.99$ ), with the amplitude and phase functions.

We may write (25) in the form

$$\psi = (\psi_1 + i\psi_2) e^{-i\sigma t},$$

in which  $\psi_1$  and  $\psi_2$  represent the in-phase and quadrature components of the flow. Then it is clear that in this  $\beta$ -plane approximation

$$(\psi_1^2 + \psi_2^2)^{\frac{1}{2}} = J_n(\gamma r) \frac{\cos}{\sin} \{n \tan^{-1}(y/x)\}$$

and

$$\tan^{-1}(\psi_2/\psi_1) = -\gamma x.$$

In order to compare the lowest mode on the hemisphere with the corresponding  $\beta$ -plane solution, figure 2 shows the 'amplitude function'  $(\psi_1^2 + \psi_2^2)^{\frac{1}{2}}$ , where  $\psi_1$  and  $\psi_2$  are the stream-functions in figure 2. It can be seen that the amplitude function has nearly circular symmetry and no nodal lines other than the boundary, just as the Bessel function

$$J_n(\gamma r) \cos \{n \tan^{-1}(\psi_2/\psi_1)\}$$

with  $n = 0$  and  $m = 1$ . Moreover, the period of the lowest mode on the sphere is 1.62 c/d compared with the frequency of the lowest  $\beta$ -plane mode which is 1.53 c/d—a difference of about 6% (see table 5).

TABLE 4. THE  $m$ TH ROOT  $z_{n,m}$  OF  $J_n(z) = 0$

$n \backslash m$	0	1	2	3	4	5	6	7	8	9	10
1	2.40	3.83	5.14	6.38	7.59	8.77	10.0	11.2	12.3	13.5	14.6
2	5.52	7.02	8.42	9.76	11.1	12.3	13.7	14.9	—	—	—
3	8.65	10.2	11.6	13.0	14.4	—	—	—	—	—	—
4	11.8	13.3	14.8	—	—	—	—	—	—	—	—
5	14.9	—	—	—	—	—	—	—	—	—	—

It will be noticed that in figure 2 the amplitude function is somewhat flattened towards the equator. This can be ascribed to the geometrical trapping effect discussed in I.

The 'phase function'  $\tan^{-1}(\psi_2/\psi_1)$  for the lowest mode is shown in figure 2. As we might expect, the phase advances at a nearly uniform rate from east to west.

Thus the lowest symmetric mode corresponds quite well with the lowest mode in a circular basin on the  $\beta$ -plane.

The computed functions  $\psi_1$ ,  $\psi_2$ ,  $(\psi_1^2 + \psi_2^2)^{\frac{1}{2}}$  and  $\tan^{-1}(\psi_2/\psi_1)$  for the lowest *antisymmetric* mode are shown in figure 7. The chief difference between these and the corresponding functions in figure 2 is the existence of a streamline  $\psi_1 = 0$  and  $\psi_2 = 0$  along the equator. The amplitude function  $(\psi_1^2 + \psi_2^2)^{\frac{1}{2}}$  therefore has a nodal line along the equator also, and the phase function  $\tan^{-1}(\psi_2/\psi_1)$  has a discontinuity of  $180^\circ$  at the equator. The mode may be compared with the lowest antisymmetric mode on the  $\beta$ -plane, in which

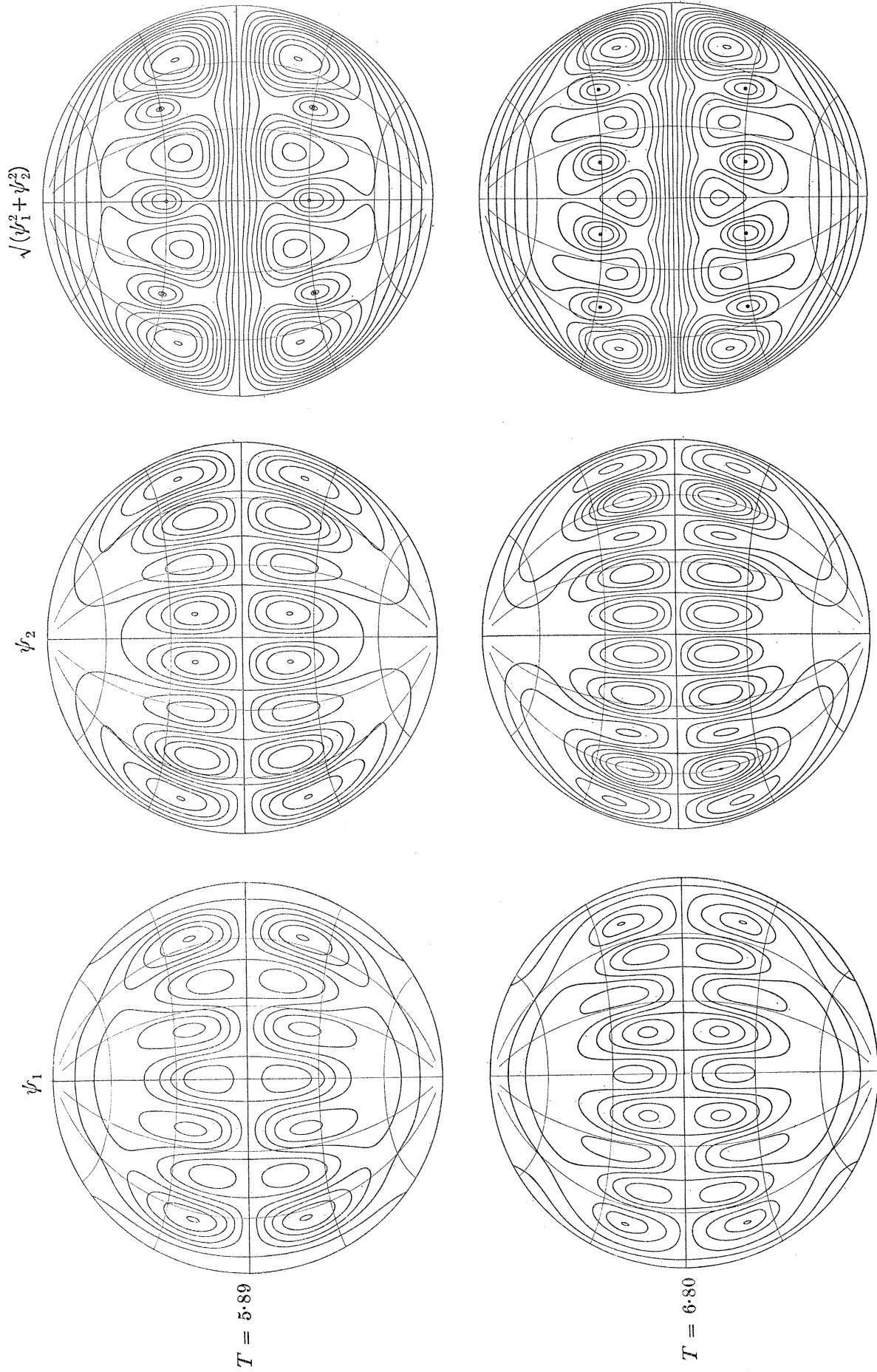
$$(\psi_1^2 + \psi_2^2)^{\frac{1}{2}} = J_1(\gamma r) \sin \chi \quad (\chi = \tan^{-1} \psi_2/\psi_1).$$

The period of the spherical mode is 3.33 d compared with 2.44 d for the  $\beta$ -plane mode. This is not so close as for the symmetric mode, perhaps because in the latter the energy is located on the whole closer to the equator.

The computed functions for the next lowest *symmetric* mode on the sphere are shown in figure 3. It will be seen that  $\psi_1$  has three main cells and  $\psi_2$  four cells. The amplitude function  $(\psi_1^2 + \psi_2^2)^{\frac{1}{2}}$  is also shown in figure 3. This now has a ridge of low values lying along the central meridian. This mode can therefore be compared to the  $\beta$ -plane mode in which

$$(\psi_1^2 + \psi_2^2)^{\frac{1}{2}} = J_1(\gamma r) \cos \chi,$$

which has a nodal diameter along  $\theta = \frac{1}{2}\pi$ . The period of this mode is 2.60 days, close to the period (2.44 d) of the corresponding  $\beta$ -plane mode.



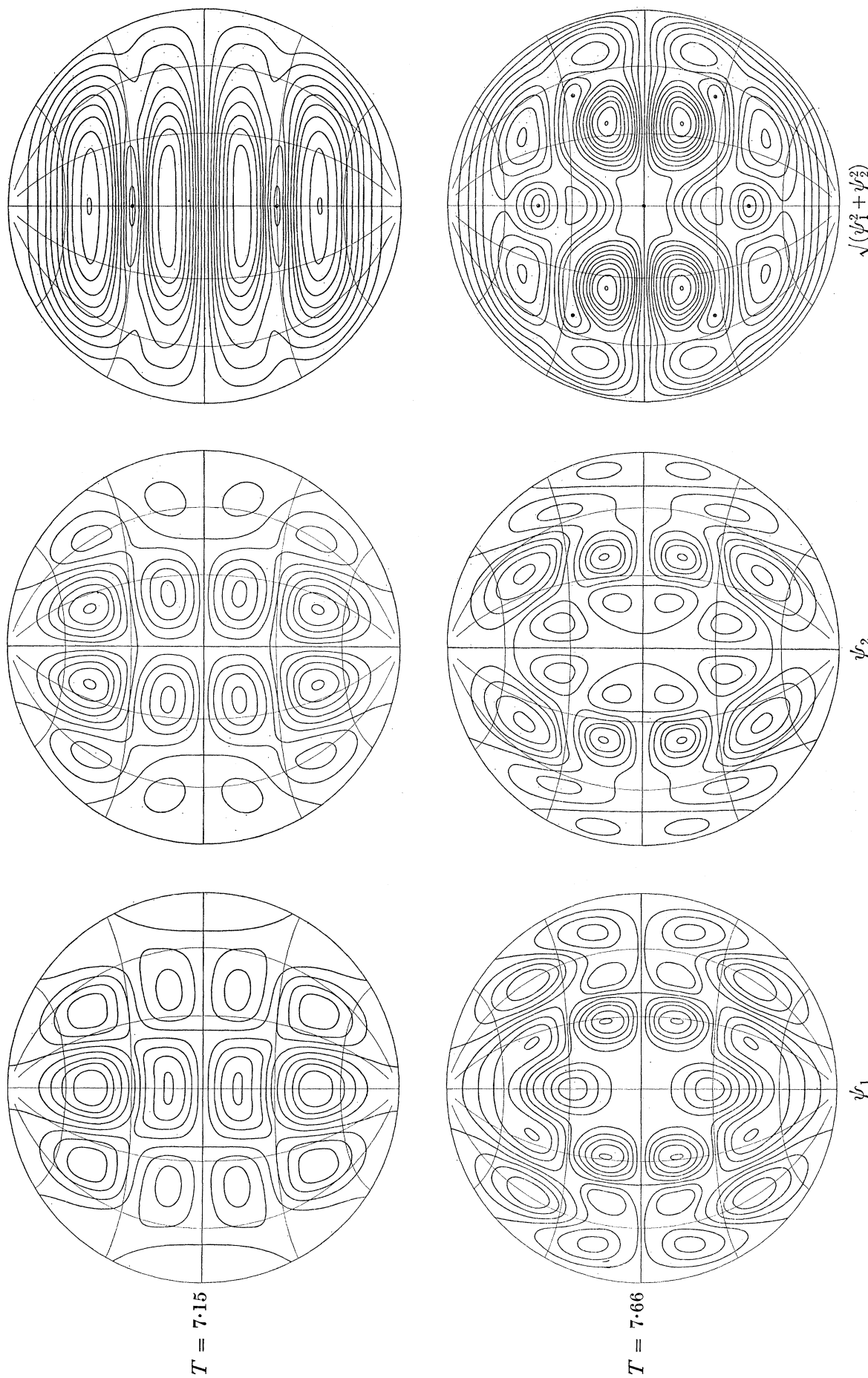
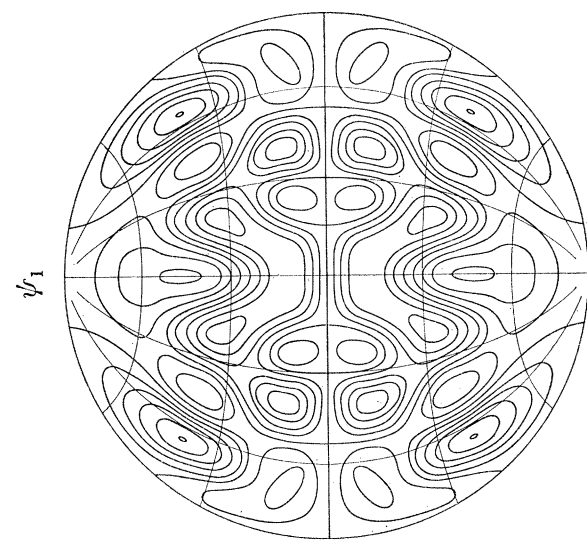
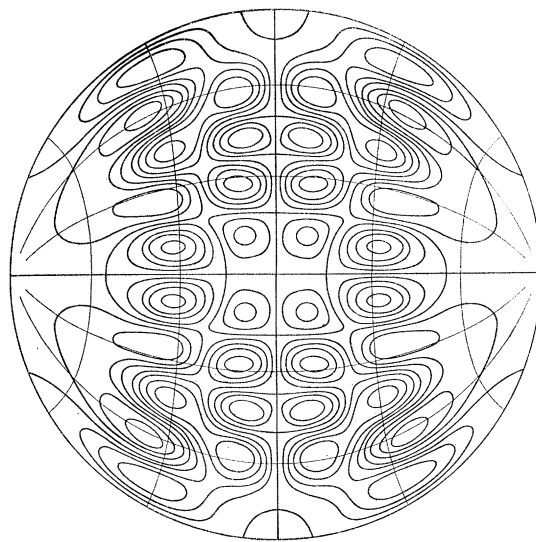
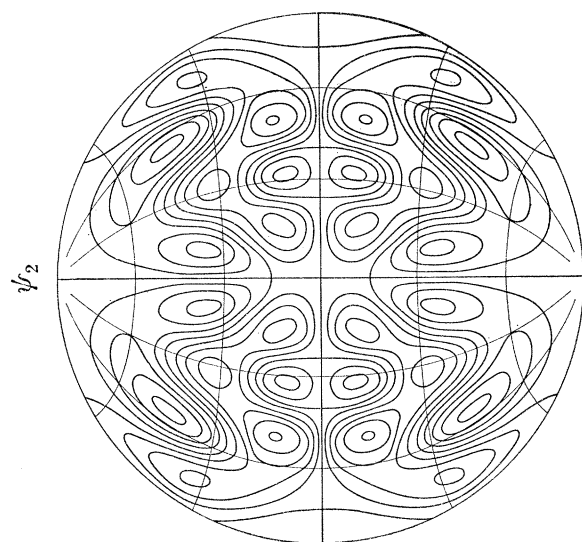
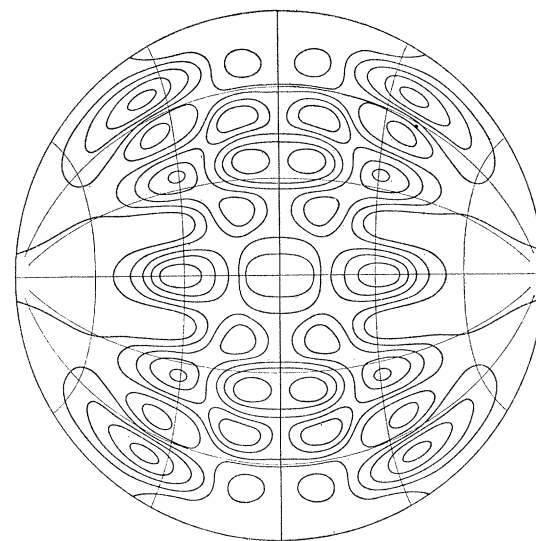


FIGURE 10. Streamlines of higher antisymmetric modes, with the corresponding amplitude functions.





$T = 8.4$



$T = 9.3$

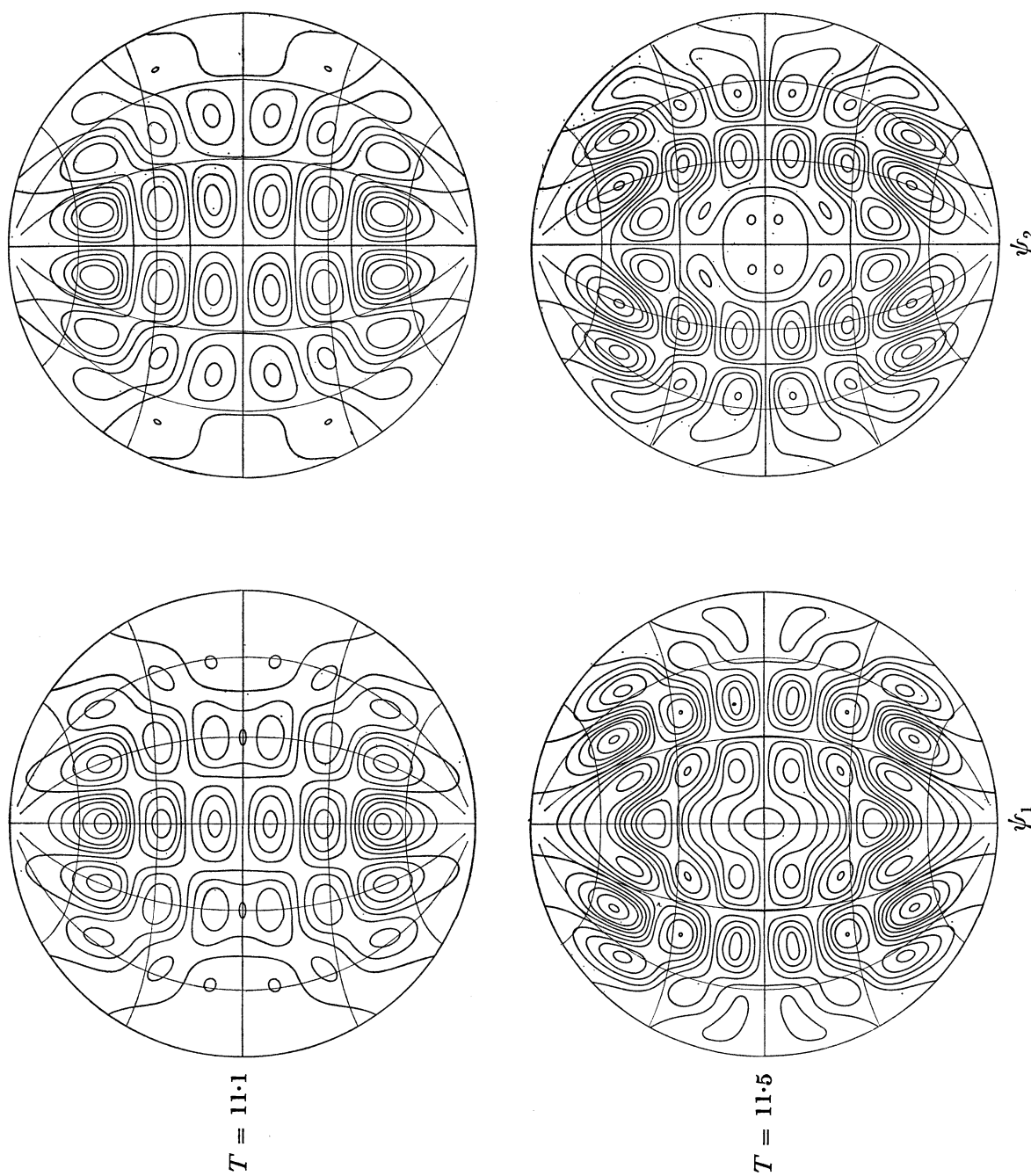




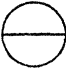
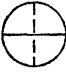




FIGURE 11. Streamlines of higher antisymmetric modes.

In this mode a new feature appears (figure 3). Where a streamline  $\psi_1 = 0$  meets a streamline  $\psi_2 = 0$  (at a simple point of intersection) there must be an amphidromic point, at which the phase progresses in a circle. A physical explanation of this may be given as follows. In the  $\beta$ -plane approximation the phases tend to progress westwards with a constant phase-velocity  $2\sigma^2/\beta$ . But on the sphere  $\beta$  is not a constant but is greater at points near the equator than near the poles. Consequently at low latitudes the phase tends to travel more slowly than in high latitudes. The existence of amphidromic points enables the phase at low latitudes to 'catch up' the phase at higher latitudes as the waves progress westwards.

From figures 4, 8 and 9, it can be seen that some of the other modes of oscillation also have amplitude functions resembling those of membrane oscillations. In table 5 the periods are compared with those of the corresponding  $\beta$ -plane approximations. The agreement between columns 1 and 4 is fairly close, especially for the symmetric modes.

TABLE 5. COMPARISON OF THE LOWEST MODES OF OSCILLATION IN A HEMISPHERICAL BASIN WITH THE CORRESPONDING MODES ON A  $\beta$ -PLANE

	$\Omega/\sigma$	nodal lines	$(n, m)$	$2z_{n,m}/\pi$
symmetric modes	1.62		(0, 1)	1.53
	2.60		(1, 1)	2.44
	3.58		(0, 2)	3.51
	4.56		(1, 2)	4.47
antisymmetric modes	3.33		(1, 1)	2.44
	4.11		(2, 1)	3.27
	4.99		(1, 2)	4.47
	5.89		(2, 2)	5.36

Higher modes do not resemble the  $\beta$ -plane approximation so well. No doubt this is partly because the controlling influence of the circular boundaries is less, and because the trapping effect, not present in the  $\beta$ -plane, is more noticeable in the higher modes.

#### 9. APPLICATION TO THE PACIFIC OCEAN

Before the present model can be applied to the real oceans, the effect of the finite depth  $h$  must be considered. As shown in II this introduces other terms into the differential equations of the motion, and gives rise, apart from the planetary waves, to gravity waves also. Nevertheless, the planetary waves can be approximated by an equation which reduces to

the spheroidal wave equation for sufficiently large wavenumber  $n$ . The terms neglected are of order  $1/n^2$ . For the Pacific Ocean  $n$  is of order 2 or 3 at least, so that in using this approximation we must expect errors of the order of 0.25 to 0.1 at most.

By use of the spheroidal wave equation it was shown that the effect of finite depth is in general to intensify the trapping of the waves towards the equator. From examining a particular example (II) it appeared that the trapping is not much more severe than the geometrical trapping due to the spherical curvature, which is already present when  $R\Omega/\sqrt{gh} \rightarrow 0$ . However, for the higher modes (longer periods) the trapping effect gives rise to a critical latitude beyond which waves of a given period cannot penetrate far.

The spheroidal wave equation can in general be approximated by the  $\beta$ -plane approximation locally, that is to say within a distance of the order of one wavelength from the central latitude. The error in the approximation is of order  $1/n$  if the central latitude is not on the equator, and of order  $1/n^2$  if it is. Thus if we are considering the symmetric oscillations the error is of order no greater than that already neglected.

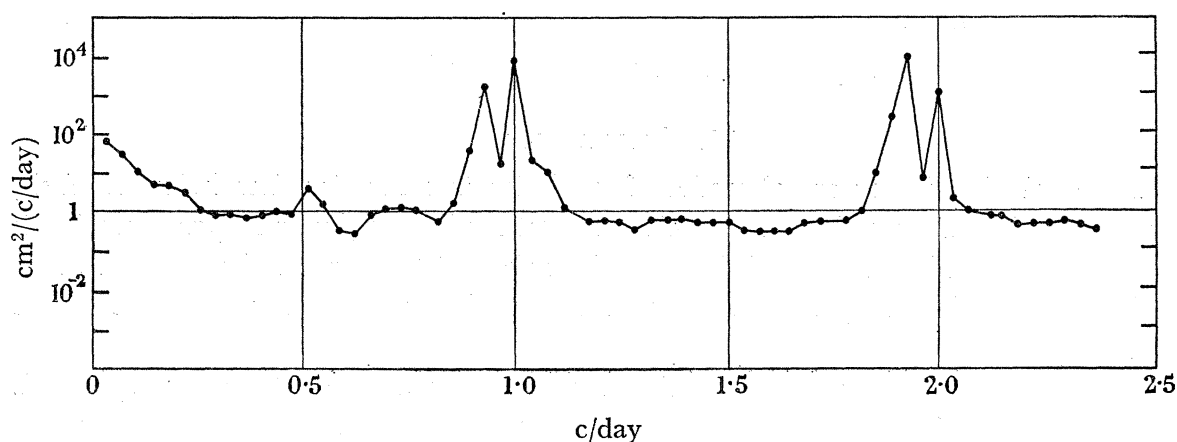


FIGURE 12. Spectrum of sea level at Honolulu, July 1938 to December 1957.  
(After Munk & Cartwright 1966.)

Hence, when considering an ocean basin of the dimensions of the Pacific Ocean, which is centred nearly on the equator and has a radius less than  $\frac{1}{2}\pi$ , it may be permissible to treat the lower modes of oscillation by a  $\beta$ -plane approximation for finite depth.

Now the  $\beta$ -plane approximation for finite depth  $h$  involves the parameter  $f^2/gh$ , where  $f$  is the local Coriolis parameter; and on the equator  $f$  vanishes, as though  $h$  were infinite. Hence, we may perhaps be able to apply the  $\beta$ -plane approximation to the lower modes of oscillation, assuming the depth infinite, as in the present paper.

In figure 12 is shown the spectrum of sea level at Honolulu, calculated by Munk & Cartwright (1966). The most obvious features of the spectrum are the peaks at the tidal frequencies of  $1\text{ c/d}$  (diurnal tide) and  $2\text{ c/d}$  (semi-diurnal tide). Apart from the gradual increase in spectral density towards low frequencies, which is characteristic of most geophysical time-series, the next most prominent feature is the peak at about  $0.5\text{ c/d}$ . This peak is certainly significant, being a much greater departure from the flat background than could be accounted for by random variations. There is no good reason to suppose it is a subharmonic of the tidal frequency, since subharmonics are not found in other tidal records.

Let us consider whether it might correspond to a mode of oscillation of the Pacific Ocean basin.

If we assume the Pacific Ocean basin to be roughly circular with a radius of 1 rad (less than  $\frac{1}{2}\pi$ ) then according to the  $\beta$ -plane approximation (26) the frequencies of oscillation ( $c/d$ ) are given

$$\sigma/\Omega = 1/z_{n,m}.$$

From table 4 the lowest mode has a frequency

$$\sigma/\Omega = 1/z_{0,1} = 0.42 c/d,$$

not far from the peak at  $0.5 c/d$  in figure 12.

The next lowest frequency corresponds to the second symmetric mode:

$$\sigma/\Omega = 1/z_{1,1} = 0.26 c/d.$$

However, this having a nodal line down the central meridian would not be likely to be observed at Honolulu. The higher modes do not necessarily have this feature, but their frequencies, all less than  $0.2 c/d$ , tend to lie very close together. If their damping is appreciable they would tend to be blurred, and so would not show up as sharp lines in the spectrum. Indeed, the rise in the observed spectral density at low frequencies may possibly be due to the amalgamation of the higher modes into a continuous background.†

## 10. CONCLUSIONS

We have calculated the normal modes of oscillation in a rotating, hemispherical shell, and have found that for at least eight of the lowest modes the  $\beta$ -plane approximation is reasonably accurate. It is suggested that a peak at about  $0.5 c/d$  in the observed spectrum of sea level at Honolulu may correspond to the lowest planetary-wave mode in the Pacific Ocean.

These conclusions suggest several directions in which future investigations might proceed. In the first place it should be possible to extend the present method of calculation of the modes of oscillation in basins of ideal shape so as to gain a more accurate estimate of the effect of horizontal divergence upon the eigenfrequencies.

Secondly, a more realistic representation of actual basins such as the Pacific Ocean might be made possible by numerical methods, on replacing the differential equation by difference equations to be satisfied at the points of a grid. In this way the effects of varying bottom topography might be included. A valuable check on the accuracy of this method would be provided by comparison of these numerical solutions in ideal cases with the solutions obtained analytically by the method described in the present paper.

Lastly, the collection and analysis of records of current velocity and surface elevation should be undertaken with a view to confirming the existence of this type of oscillation in ocean basins.

## APPENDIX. AN ALTERNATIVE METHOD

The following independent method was used as a valuable check on the eigenfrequencies. However, the method has some interest in itself. It involves transforming the pole of coordinates to the centre of the basin, lying on the equator; hence it could be adapted to other circular basins centred on the equator, but of radius different from  $\frac{1}{2}\pi$ .

† A short calculation shows that the number of modes contained within a given small frequency interval increases proportionally to  $\sigma^{-3}$  as  $\sigma \rightarrow 0$ .

If the new coordinates are chosen suitably, the equator will be given by  $\phi = 0$  (in the eastward direction) and the boundary of the hemisphere by  $\theta = \frac{1}{2}\pi$ . When transformed to the new coordinates, equation (1) becomes

$$\frac{\partial}{\partial t}(\nabla^2\psi) + 2\Omega \left( \sin\theta \cos\phi \frac{\partial}{\partial\mu} + \cot\theta \sin\phi \frac{\partial}{\partial\phi} \right) \psi = 0, \quad (30)$$

where  $\mu = \cos\theta$ . The boundary condition becomes

$$\psi = 0 \quad \text{when} \quad \theta = \frac{1}{2}\pi. \quad (31)$$

Now let  $\psi$  be expanded in the form

$$\psi = \sum_{m=0}^{\infty} \sum_{n=m}^{\infty} P_n^m(\mu) [K_m C_n^m \cos m\phi + D_n^m \sin m\phi], \quad (32)$$

where  $K_m = 1$  when  $m \neq 0$  and  $K_0 = \frac{1}{2}$ . Since the function is defined only over  $0 \leq \mu \leq 1$  we may assume that, in the summation with respect to  $n$ ,  $(n-m)$  takes only odd integer values. This incidentally ensures that each term of the series vanishes on the boundary. Substitution in the differential equation (30) now gives

$$\begin{aligned} & i\sigma \sum_{m=0}^{\infty} \sum_{n=m+1}^{\infty} n(n+1) P_n^m [K_m C_n^m \cos m\phi + D_n^m \sin m\phi] \\ & + 2\Omega \sum_{m=0}^{\infty} \sum_{n=m+1}^{\infty} \left\{ (1-\mu^2)^{\frac{1}{2}} \frac{dP_n^m}{d\mu} [K_m C_n^m \cos\phi \cos m\phi + D_n^m \cos\phi \sin m\phi] \right. \\ & \quad \left. + \frac{m\mu}{(1-\mu^2)^{\frac{1}{2}}} P_n^m [-K_m C_n^m \sin\phi \sin m\phi + D_n^m \sin\phi \cos m\phi] \right\} = 0. \end{aligned} \quad (33)$$

Now from the definition of  $P_n^m(\mu)$  it follows that when  $m \geq 0$

$$(1-\mu^2)^{\frac{1}{2}} \frac{dP_n^m}{d\mu} = P_n^{m+1} - \frac{m\mu}{(1-\mu^2)^{\frac{1}{2}}} P_n^m; \quad (34)$$

so that the expression in curly brackets becomes

$$\begin{aligned} & \left\{ K_m C_n^m \left[ P_n^{m+1} \cos\phi \cos m\phi - \frac{m\mu}{(1-\mu^2)^{\frac{1}{2}}} P_n^m \cos(m-1)\phi \right] \right. \\ & \quad \left. + D_n^m \left[ P_n^{m+1} \cos\phi \sin m\phi - \frac{m\mu}{(1-\mu^2)^{\frac{1}{2}}} P_n^m \sin(m-1)\phi \right] \right\}. \end{aligned} \quad (35)$$

But when  $m \geq 1$  we have also

$$\frac{2m\mu}{(1-\mu^2)^{\frac{1}{2}}} P_n^m = P_n^{m+1} + (n+m)(n-m+1) P_n^{m-1}. \quad (36)$$

Hence (35) becomes

$$\begin{aligned} & \left\{ \frac{1}{2} C_n^m [P_n^{m+1} \cos(m+1)\phi - (n+m)(n-m+1) P_n^{m-1} \cos(m-1)\phi] \right. \\ & \quad \left. + \frac{1}{2} D_n^m [P_n^{m+1} \sin(m+1)\phi - (n+m)(n-m+1) P_n^{m-1} \sin(m-1)\phi] \right\}. \end{aligned} \quad (37)$$

When  $m = 0$  (35) is clearly  $\frac{1}{2} C_n^0 P_n^1 \cos\phi$ .

So equation (33) becomes

$$\begin{aligned} & i\sigma \sum_{m=0}^{\infty} \sum_{n=m+1}^{\infty} n(n+1) P_n^m [K_m C_n^m \cos m\phi + D_n^m \sin m\phi] \\ & + \Omega \sum_{m=1}^{\infty} \sum_{n=m+1}^{\infty} \{C_n^m [P_n^{m+1} \cos(m+1)\phi - (n+m)(n-m+1) P_n^{m-1} \cos(m-1)\phi] \\ & \quad + D_n^m [P_n^{m+1} \sin(m+1)\phi - (n+m)(n-m+1) P_n^{m-1} \sin(m-1)\phi]\} \\ & + \Omega \sum_{n=1}^{\infty} C_n^0 P_n^1 \cos \phi = 0. \end{aligned} \quad (38)$$

Clearly the coefficients of  $\cos m\phi$  involve only the  $C_n^m$ , and the coefficients of  $\sin m\phi$  involve only the  $D_n^m$ . The solutions involving the  $C_n^m$  are symmetric about the equator ( $\phi = 0$ ) and the solutions involving the  $D_n^m$  are antisymmetric about the equator, i.e. for them the equator is a streamline.

To investigate the symmetric modes, let us equate to zero the coefficients of  $\cos m\phi$ , for  $m = 0, 1, 2, \dots$ . Then we obtain

$$i\sigma \sum_{n=m+1}^{\infty} n(n+1) C_n^m P_n^m + \Omega \sum_{n'=m}^{\infty} [C_{n'}^{m-1} - (n'+m+1)(n'-m) C_{n'}^{m+1}] P_{n'}^m = 0 \quad (m = 0, 1, 2, \dots), \quad (39)$$

where by convention  $C_n^{-1} = 0$  and  $C_n^{m+1} = 0$ . Now in the above summations  $(n'-m)$  is always even so that the  $P_{n'}^m$  on the right-hand side are of different type to the  $P_n^m$  on the left. Accordingly we expand  $P_{n'}^m$  in the form

$$P_{n'}^m = G(n', n) P_n^m \quad (0 < \mu < 1), \quad (40)$$

where the  $G(n', n)$  are constant coefficients and  $(n-m)$  is always odd. Then substituting in equation (39) and equating to zero the coefficients of  $P_n^m$  we have

$$i\sigma n(n+1) C_n^m + \Omega \sum_{n'=m}^{\infty} [C_{n'}^{m-1} - (n'+m+1)(n'-m) C_{n'}^{m+1}] G(n', n) = 0. \quad (41)$$

To find the coefficients  $G(n', n)$  in (40) let us multiply by  $P_{n'}^m$ , where  $(n''-m)$  is odd (i.e.  $n''$  is of the same parity as  $n$ ) and integrate over  $0 < \mu < 1$ . Since the product  $P_n^m P_{n'}^m$  is an even function of  $\mu$ , the integral over  $0 < \mu < 1$  is exactly half the integral taken over  $-1 < \mu < 1$ . By equation (9), all the terms on the right then vanish, except those for which  $n'' = n$ , and consequently we have from (9)

$$\int_0^1 P_n^m P_{n'}^m d\mu = G(n', n'') \frac{1}{2n''+1} \frac{(n''-m)!}{(n''+m)!}.$$

So on replacing  $n''$  by  $n$  we find

$$G(n', n) = (2n+1) \frac{(n-m)!}{(n+m)!} \int_0^1 P_{n'}^m P_n^m d\mu. \quad (42)$$

The integral on the right can be evaluated from the identity

$$\frac{d}{d\mu} \left[ (1-\mu^2) \left\{ P_{n'}^m \frac{dP_n^m}{d\mu} - P_n^m \frac{dP_{n'}^m}{d\mu} \right\} \right] + (n'-n)(n+n'+1) P_{n'}^m P_n^m = 0$$

(which follows from the differential equations for  $P_n^m$  and  $P_n^{m'}$ ). Integrating over  $0 < \mu < 1$  we have

$$\left\{ P_n^{m'} \frac{dP_n^m}{d\mu} - P_n^m \frac{dP_n^{m'}}{d\mu} \right\} + (n' - n)(n + n' + 1) \int_0^1 P_n^{m'} P_n^m d\mu = 0,$$

and so, since  $(n' - n) \neq 0$ ,

$$\int_0^1 P_n^{m'} P_n^m d\mu = \frac{1}{(n - n')(n + n' + 1)} \left[ P_n^{m'} \frac{dP_n^m}{d\mu} - P_n^m \frac{dP_n^{m'}}{d\mu} \right]_{\mu=0}. \quad (43)$$

But since  $(n - m)$  is odd,  $P_n^m$  vanishes at  $\mu = 0$ ; while from (34) we have

$$\left( \frac{dP_n^m}{d\mu} \right)_{\mu=0} = (P_n^{m+1})_{\mu=0}.$$

Hence we have simply

$$\int_0^1 P_n^{m'} P_n^m d\mu = \frac{1}{(n - n')(n + n' + 1)} (P_n^{m'} P_n^{m+1})_{\mu=0}. \quad (44)$$

Combining (42) and (44) we obtain

$$G(n', n) = \frac{(2n + 1)}{(n - n')(n + n' + 1)} \frac{(n - m)!}{(n + m)!} (P_n^{m'} P_n^{m+1})_{\mu=0}. \quad (45)$$

It is easily shown that when  $m \geq 0$

$$P_n^m(0) = \begin{cases} 0 & (n - m) \text{ odd,} \\ \frac{(-1)^{\frac{1}{2}(n-m)} (n + m)!}{2^n [\frac{1}{2}(n - m)]! [\frac{1}{2}(n + m)]!} & (n - m) \text{ even.} \end{cases} \quad (46)$$

Substituting from (45) into (41) we have now

$$-\frac{i\sigma}{\Omega} \frac{n(n+1)}{(2n+1)} \frac{(n+m)!}{(n-m)!} C_n^m = \sum_{n'=m}^{\infty} \frac{C_n^{m-1} - (n' + m + 1)(n' - m) C_n^{m+1}}{(n - n')(n + n' + 1)} (P_n^{m'} P_n^{m+1})_{\mu=0}, \quad (47)$$

when  $m = 0, 1, 2, \dots$ . These simultaneous equations have now to be solved for the eigenvalues  $(\sigma/\Omega)$  and the constants  $C_n^m$ .

The equations may be thrown into more convenient form if we introduce the symbol  $\zeta(m, m')$  defined by

$$\zeta(m, m') = \begin{cases} 1 & (m - m') = \pm 1 \\ 0 & \text{otherwise.} \end{cases}$$

Then we have

$$\begin{aligned} \sum_{m'=-\infty}^{\infty} \zeta(m, m') C_n^{m'} (P_n^{m'+1} P_n^{m+1})_{\mu=0} &\equiv C_n^{m-1} (P_n^m P_n^{m+1})_{\mu=0} + C_n^{m+1} (P_n^{m+2} P_n^{m+1})_{\mu=0} \\ &\equiv [C_n^{m-1} - (n' - n)(n' + m + 1) C_n^{m+1}] (P_n^m P_n^{m+1})_{\mu=0} \end{aligned}$$

by (46). So (47) can be written

$$-\frac{i\sigma}{2\Omega} \frac{n(n+1)}{n + \frac{1}{2}} \frac{(n+m)!}{(n-m)!} C_n^m = \sum_{m'=0}^{n'-1} \sum_{n'=m}^{\infty} \frac{\zeta(m, m')}{(n - n')(n + n' + 1)} C_n^{m'} (P_n^{m'+1} P_n^{m+1})_{\mu=0}, \quad (48)$$



where  $m = 0, 1, 2, \dots$ ;  $m' = 0, 1, 2, \dots$ , and  $(n-m)$  is odd. Since  $(n'-m)$  is even, and  $\zeta(m, m')$  vanishes except when  $(m-m') = \pm 1$ ,  $(n'-m')$  can be assumed to be odd also. To make the system of equations completely symmetrical in  $(m, n)$ ,  $(m', n')$ , write

$$\left[ \frac{n(n+1)(n+m)!}{(n+\frac{1}{2})(n-m)!} \right]^{\frac{1}{2}} C_n^m = E_n^m. \quad (49)$$

Then (48) becomes

$$\frac{\sigma}{2\Omega} E_n^m = \sum_{m'} \sum_{n'} iS \begin{pmatrix} m & m' \\ n & n' \end{pmatrix} E_{n'}^{m'}, \quad (50)$$

where

$$S \begin{pmatrix} m & m' \\ n & n' \end{pmatrix} = \left[ \frac{(n+\frac{1}{2})(n-m)!}{n(n+1)(n+m)!} \frac{(n'+\frac{1}{2})(n'-m')!}{n'(n'+1)(n'+m')!} \right]^{\frac{1}{2}} \frac{\zeta(m, m')}{(n-n')(n+n'+1)} (P_n^{m+1} P_{n'}^{m'+1})_{\mu=0}. \quad (51)$$

Now  $S$  is clearly antisymmetric in  $\begin{pmatrix} m \\ n \end{pmatrix}$ ,  $\begin{pmatrix} m' \\ n' \end{pmatrix}$ , and so the set of equations (50) is Hermitian.

From this point on, the solution of (50) proceeds in a similar way to the solution of (17).

We construct a real symmetric matrix  $T \begin{pmatrix} m & r \\ n & s \end{pmatrix}$  whose eigenvalues are the squares of the eigenvalues of  $iS$ ; by taking the square root we find  $\sigma/2\Omega$ . From the eigenvectors  $E_n^m$  we calculate  $E_s^r$  and so  $C_n^m$  and  $C_s^r$  by (49).

It will be seen that the equations for the coefficients of the antisymmetric modes are identical with those for the symmetric modes, except that the first row and the first column of the matrix are omitted.

One proceeds, as in the previous method, by truncating the infinite matrix  $S$  after a finite number  $\frac{1}{2}k(k+1)$  of rows and columns, where  $k$  is a positive integer. Successive values of  $k$  give successive, and mutually independent, approximations to the eigenvalues and eigenvectors.

The notable result of this calculation was that at each value of  $k$  the resulting eigenfrequencies were identical, to six decimal places, with those calculated by the first method,† for the same value of  $k$ . This strongly suggests that not only are the infinite matrices algebraically equivalent, that is, they have the same eigenvalues, but that the truncated matrices are equivalent also.

A proof of the equivalence of the truncated matrices may be sketched as follows. If we group together all those spherical harmonics in the original expansion (3) which are of degree  $k$  and denote their sum by  $U_k$  we may write

$$\psi = \sum_{k=0}^{\infty} U_k(\theta, \phi) e^{-i\sigma t}. \quad (52)$$

Similarly, if we denote the spherical harmonics in the expansion (32) by  $V_k(\theta', \phi')$ , where  $\theta'$  and  $\phi'$  denote the new coordinates we have

$$\psi = \sum_{k=0}^{\infty} V_k(\theta', \phi') e^{-i\sigma t}. \quad (53)$$

† Except that when  $k = 8$  (the highest approximation) and  $\sigma/\Omega < 0.01$ , the antisymmetric modes showed some discrepancies in the fourth decimal place. The limitation in accuracy appeared to arise in calculating the elements of  $S$ , not in the resolution of the matrix.

Now the expansion of a function, defined over the whole sphere, in terms of all the spherical harmonics is unique; the same must also be true of the expansion of a function, defined over only half the sphere and extended by reflexion in the boundary, in terms of the 'odd' harmonics only, that is, those harmonics which vanish on the boundary. Further a spherical harmonic of a given degree  $k$  with pole at one point may always be expressed as a finite sum of harmonics of the same degree  $k$  with pole at some other point. It follows that

$$U_k(\theta, \phi) \equiv V_k(\theta', \phi'). \quad (54)$$

Now the derivatives  $\partial U_k/\partial\phi$ , say, have themselves been expressed as infinite series in the  $U_k$ . The series were then truncated for the purpose of computation. By the same argument we see that the *truncated* series for  $\partial U_k(\theta, \phi)/\partial\phi$ , expressed in terms of the  $U_k$ , must be identical with the *truncated* series for  $\partial V_k(\theta', \phi')/\partial\phi$  in terms of the  $U_k$  (or  $V_k$ ). Hence the truncated systems of equations are equivalent also, that is to say the truncated matrices are equivalent.

In am indebted to my colleague, Mr J. Crease, for many useful discussions on the algebraic and computational aspects of this problem. The spectrum of sea level at Honolulu is quoted from a forthcoming paper by Walter H. Munk and David Cartwright, by kind permission of the authors.

#### REFERENCES

- Arons, A. B. & Stommel, H. 1956 A  $\beta$ -plane analysis of free periods of the second class in meridional and zonal oceans. *Deep-Sea Res.* **4**, 23–31.
- Ashour, A. A. 1964 On some formulae for integrals of associated Legendre functions. *Quart. J. Mech. Appl. Math.* **17**, 513–523.
- Givens, W. 1954 Numerical computation of the characteristic values of a real symmetric matrix. *Oak Ridge Nat. Lab. Rep.* no. 1574.
- Goldsbrough, G. R. 1913 The dynamical theory of the tides in a polar basin. *Proc. Lond. Math. Soc.* (2), **14**, 31–66.
- Goldsbrough, G. R. 1914 The dynamical theory of the tides in a zonal ocean. *Proc. Lond. Math. Soc.* (2), **14**, 207–229.
- Goldsbrough, G. R. 1929 The tides in oceans on a rotating globe, part III. *Proc. Roy. Soc. A*, **126**, 1–15.
- Goldsbrough, G. R. 1933 The tides on a rotating globe, part IV. *Proc. Roy. Soc. A*, **140**, 241–253.
- Hoiland, E. 1950 On horizontal motion in a rotating fluid. *Geofys. Publ.* no. 10, 26 pp.
- Hough, S. S. 1898 On the application of harmonic analysis to the dynamical theory of the tides. Part II. On the general integration of Laplace's tidal equations. *Phil. Trans. A*, **191**, 139–185.
- Householder, A. S. 1958 Unitary triangularisation of a non symmetric matrix. *J. Ass. Comp. Mach.* **5**, 339–342.
- Longuet-Higgins, M. S. 1964a Planetary waves on a rotating sphere. *Proc. Roy. Soc. A*, **279**, 446–473.
- Longuet-Higgins, M. S. 1964b On group velocity and energy flux in planetary wave motions. *Deep-Sea Res.* **11**, 35–42.
- Longuet-Higgins, M. S. 1965 Planetary waves on a rotating sphere. II. *Proc. Roy. Soc. A*, **284**, 40–54
- Longuet-Higgins, M. S. & Crease, J. (MS. in preparation). On the integrated product of two associated Legendre functions.
- MacRobert, T. M. 1926 Expansions in a series of spherical harmonics. *Proc. Edinb. Math. Soc.* **42**, 88–92.
- Munk, W. H. & Cartwright, D. E. 1966 Tidal spectroscopy and prediction. *Phil. Trans. A*, **259**, 533–581.

- Proudman, J. 1920 On the dynamical equations of the tides. *Proc. Lond. Math. Soc.* (2), **18**, 1–68.
- Proudman, J. & Doodson, A. T. 1936 Tides in oceans bounded by meridians. *Phil. Trans. A*, **235**, 273–342.
- Rattray, M. 1964 Time-dependent motion in an ocean: a unified, two-layer beta-plane approximation. *Studies in oceanography*. Tokyo: Geophys. Inst., Tokyo Univ. (560 pp.).
- Whittaker, E. T. & Watson, G. N. 1927 *A course of modern analysis*, 4th ed. (608. pp.). Cambridge University Press.
- Wilkinson, J. H. 1958 Calculation of the eigenvectors of codiagonal matrices. *Computer J.* **1**, 90–96.